The EUMETSAT Network of Satellite Application Facilities

ROM SAF
Radio Occultation Meteorology

ROM SAF CDOP-2

Visiting Scientist Report 23:

Feasibility of generating long-term RO refractivity climatologies without using statistical optimization

Julia Danzer

Danish Meteorological Institute (DMI)
European Centre for Medium-Range Weather Forecasts (ECMWF)
Institut d'Estudis Espacials de Catalunya (IEEC)
Met Office (METO)

Ref: SAF/ROM/DMI/REP/VS23/001
Version: 1.0
Date: 21 March 2014

DOCUMENT AUTHOR TABLE

	Author(s)	*Function*	*Date*	*Comment*
Prepared by:	Julia Danzer	ROM SAF Visiting Scientist	28/02/2014	
Reviewed by (internal):	Hans Gleisner	ROM SAF Scientist	18/03/2014	
Approved by:	Kent B. Lauritsen	ROM SAF Project Manager	18/03/2014	

DOCUMENT CHANGE RECORD

Issue/Revision	*Date*	*By*	*Description*
Draft 1	27/01/2014	JD	First draft
Draft 2	10/02/2014	JD	Second draft
Final	28/02/2014	JD	Final version
1.0	21/03/2014	JD	Final version (after fixing PDF file)

VS Author

This VS study was carried out by Dr. Julia Danzer, Wegener Center, Univ. of Graz, Austria; email: julia.danzer@uni-graz.at

VS Duration

The VS study was performed at the home institute during October 2013 to February 2014 and included a ten days visit in October to the Danish Meteorological Institute, Copenhagen, Denmark.

ROM SAF

The Radio Occultation Meteorology Satellite Application Facility (ROM SAF) is a decentralised processing center under EUMETSAT which is responsible for operational processing of GRAS radio occultation data from the Metop satellites and radio occultation (RO) data from other missions. The ROM SAF delivers bending angle, refractivity, temperature, pressure, and humidity profiles in near-real time and offline for NWP and climate users. The offline profiles are further processed into climate products consisting of gridded monthly zonal means of bending angle, refractivity, temperature, humidity, and geopotential heights together with error descriptions.

The ROM SAF also maintains the Radio Occultation Processing Package (ROPP) which contains software modules that will aid users wishing to process, quality-control and assimilate radio occultation data from any radio occultation mission into NWP and other models.

The ROM SAF Leading Entity is the Danish Meteorological Institute (DMI), with Cooperating Entities: i) European Centre for Medium-Range Weather Forecasts (ECMWF) in Reading, United Kingdom, ii) Institut D'Estudis Espacials de Catalunya (IEEC) in Barcelona, Spain, and iii) Met Office in Exeter, United Kingdom. To get access to our products or to read more about the ROM SAF please go to: http://www.romsaf.org

Intellectual Property Rights

Contents

Executive summary

The goal of this study is to analyze a new approach which circumvents Statistical Optimization (SO) in the retrieval of geophysical parameters from bending angle profiles. The approach is designed for the investigation of climatologies, while the standard approach employing the SO, is still needed for generating individual profiles.

The idea is to shift the averaging procedure to bending angle space, calculating monthly mean bending angle climatologies, which are then processed through an Abel transformation to obtain monthly mean refractivity climatologies.

In a first study Gleisner and Healy (2013) tested the approach on Constellation Observing System for Meteorology, Ionosphere, and Climate (COSMIC) satellite data. In order to exploit the full range of available Radio Occultation (RO) data, the usage of CHAllenging Mini-Satellite Payload (CHAMP) data is also required. The CHAMP satellite mission provides a reduced number of occultation events and increased level of noise. As a consequence, the main research question was, if the average bending angle approach is also applicable to CHAMP data.

The study focused on two main areas. First, to perform a study of bending angle averages built from CHAMP data. Their variations with altitude and latitude are studied, the differences relative to co-located European Centre for Medium-Range Weather Forecasts (ECMWF) data analyzed, mean and medians are investigated and different realizations of bending angle averages are compared. The objective is to find a suitable CHAMP bending angle average, which can be forwarded through the Abel transformation.

Secondly, refractivity climatologies from average bending angles are analyzed. They are compared to the standard retrieval from the Danish Meteorological Institute (DMI), to ECMWF analysis data and to COSMIC data sets, on a longer time scale.

The results showed that bending angle averages are best built from a combination of mean and median values, excluding large single bending angle profile outliers from the averaging. The main firm conclusion was that the average bending angle approach can be applied to CHAMP data as well. The resulting refractivity climatologies from CHAMP data showed to be practically identical to the standard retrieval at the DMI below altitudes of 35 km. Between 35 km to 50 km the differences between the two retrieval methods started to increase up to about 2%. Furthermore, at high latitudes and altitudes and winter conditions, the new approach showed even smaller biases than the standard retrieval towards ECMWF analysis data.

1 Introduction

Global Positioning System (GPS) Radio Occultation (RO) measurements are a valuable source of information for weather prediction as well as climate monitoring. The measurements are available usually to about 80 km altitude. They provide geophysical information with high quality and high vertical resolution mainly in the region of the Upper Troposphere–Lower Stratosphere (UTLS) (between about 5 km to 25 km), see e.g., Kursinski et al. (1997). At higher altitudes the measurement noise increases and becomes comparable to or even exceeds the bending angle signal.

The standard procedure to retrieve refractivity from noisy bending angles consists of a combination of smoothing and merging of the observed bending angle profiles with *a priori* information. The background model is commonly chosen from either a climatology, such as Mass Spectrometer and Incoherent Scatter Radar (MSIS), or from numerical weather prediction models, such as European Centre for Medium-Range Weather Forecasts (ECMWF). In this so-called Statistical Optimization (SO), single bending angle profiles are propagated through an Abel transformation (Fjeldbo et al. 1971), to obtain refractivity profiles. Since the Abel transformation involves an integral over infinity, an extrapolation of the finite bending angle signal is also necessary. Having obtained refractivity, atmospheric parameters such as density, pressure or temperature can be calculated after some processing steps. If the focus of interest is to study climatologies, statistical analysis usually is performed directly on the climate parameters to generate monthly mean climate data.

Recent studies within the *ROtrends* collaboration have shown that this upper-level bending angle initialization may be a source of structural uncertainties for the climate data products (Steiner et al. 2013). The processing centers use different methods and background information for their SO, which leads to differences in the climate data products mainly above 25 km.

In a new approach (Ao et al. 2012; Gleisner and Healy 2013) it has been suggested to perform the statistical analysis in bending angle space. This has the advantage to suppress the noise by averaging over a large number of profiles and it raises the altitude to which observational data can be used. Via an Abel transformation mean refractivity profiles can be directly derived from mean bending angle profiles. This so-called average bending angle approach is primarily designed for the generation of climatologies.

The recent studies tested the approach by focusing on Constellation Observing System

for Meteorology, Ionosphere, and Climate (COSMIC) data. However, when aiming long-term climate data products the use of CHAllenging Mini-Satellite Payload (CHAMP) data from 2001 to mid-2006 is also required. CHAMP data is considerably noisier than COSMIC data. An illustrative comparison of different noise levels for different satellite missions is given in the recently published report by Schwärz et al. (2013), in Fig. 1.8. They compare daily bending angle noise from 2001 to 2012, for seven different satellites, amongst which are the CHAMP satellite and the COSMIC satellite system. In their plot they show a clear enhancement of the magnitude of noise in case of studying CHAMP data compared to COSMIC satellite data. Regarding the worse data quality for CHAMP data and the reduced number of occultation events, it is a valid question if the average bending angle approach can be applied for this mission as well. Particularly I analyzed the questions:

- Does the average bending angle approach (monthly averages) work for CHAMP data, despite the higher noise level and the reduced number of profiles per month?
- How is it best to estimate monthly means in the case of CHAMP data?
  - I studied zonal mean bending angles, median bending angles, combinations of mean and median bending angle profiles.
  - Is an additional quality control in bending angle space for the more noisy CHAMP data necessary?
- Within the *ROtrends* collaborative studies it has been shown that the bending angle initialization used until recently in the standard retrieval scheme at Danish Meteorological Institute (DMI) may exhibit biases during winter conditions at high altitudes and high latitudes. One of the research questions is if the initialization can be improved for climate data using the new average bending angle approach.[1]
- Finally, I did a comparison of CHAMP and COSMIC satellite data with standard retrieval (single profile processing with SO), new retrieval (average bending angle approach), and to co-located ECMWF profiles. The following questions were analyzed:
  - How do the two procedures compare with ECMWF data? What biases are introduced due to SO, and what new biases are introduced due to the average bending angle approach?

[1] At the level of single refractivity profiles, DMI is addressing this by algorithm improvements and by using the so-called Bending Angle Radio Occultation Climatology (BAROCLIM) spectral model as their a priori information (Foelsche and Scherllin-Pirscher 2011; Scherllin-Pirscher 2013) for the SO.

- Can the climatology produced with the average bending angle approach used as a reference to other climatologies generated by the standard retrievals from different processing centers?
- Which retrieval method produces more similar results between CHAMP and COSMIC data sets? The new approach or the standard inversion?
- Is there a systematic difference between CHAMP and COSMIC satellite data?

2 Data Sets

The study focuses on occultation events observed by the CHAMP single satellite mission from September 2001 until September 2008. As a comparison, satellite data from the COSMIC six satellite constellation is studied in an overlap period from September 2006 until December 2007. At the University Corporation for Atmospheric Research / Cosmic Data Analysis and Archive Center (UCAR/CDAAC) database excess phase profiles and precise orbit information were retrieved, and further processed into bending angle and refractivity profiles at the Radio Occultation Meteorology (ROM) Satellite Application Facility (SAF), which is a RO processing center under the European Organisation for the Exploitation of Meteorological Satellites (EUMETSAT), hosted by the DMI, using the Radio Occultation Processing Package (ROPP) software as their retrieval package.

In this study, the bending angle and refractivity profiles are analyzed on a monthly basis for 10° latitudinal bins (Chapter 4), leading to between about 3500 to 5500 profiles per month in case of CHAMP data, and about 50000 to 65000 profiles per month for COSMIC data, after several steps of quality screening.

Furthermore co-located ECMWF refractivity and bending angle profiles from ECMWF analysis data are studied on 10° latitudinal bins and used as a reference for the monthly mean profiles. The used analysis data fields are studied on a T42L91 resolution, since the T42 horizontal resolution matches the resolution of RO data (∼300 km). Until January 2006 they are given on 60 vertical levels (L60), after that the ECMWF switched to 91 vertical levels (L91). Furthermore, in December 2006 the ECMWF started to assimilate GPS RO data into the analysis fields.

3 Processing of data

The production of geophysical parameters from Global Navigation Satellite System (GNSS) RO measurements requires a retrieval chain described in detail by Kursinski et al. (1997). In the retrieval an Abel transformation occurs, relating the refractive index n to the bending angle α, through,

$$\ln n(x) = \frac{1}{\pi} \int_x^\infty \frac{\alpha(a)}{\sqrt{a^2 - x^2}} da \ , \tag{3.1}$$

where a is the impact parameter and $x = nr$, with r being the radius of a point on the ray path. The integral over infinity arises a problem, since observational data has a limit in altitude to about 80 km. Hence an extrapolation to infinity becomes necessary. Furthermore the measurement noise grows in magnitude with increasing altitude. The simplest approach is to replace noisy bending angles by a smooth model based bending angle, based on extrapolation of less noisy measurements or a climatological model. More advanced is not only to do an extrapolation step and merge noisy bending angles with a priori information, but to also combine it with a smoothing step above a certain altitude (usually above about 40 km). This is referred to SO, where a statistically optimized bending angle is obtained, i.e.,

$$\alpha = \alpha_b + \mathbf{K}(\alpha_O - \alpha_b) \ , \tag{3.2}$$

yielding the optimized bending angle α. α_O and α_b are the observed and the background bending angle, respectively. $\mathbf{K}$ is the gain matrix, which can be written in terms of error covariance matrices for the observed and background bending angle profiles. Using the statistically optimized bending angle for the Abel transformation, refractivity profiles can be calculated. Continuing from refractivity, it is possible to retrieve after some following processing steps, the atmospheric parameters of the neutral atmosphere, such as, density, pressure, temperature, see e.g., Fig. 4 in Steiner et al. (2001) and in detail Kursinski et al. (1997). When comparing the results of different processing centers, discrepancies in the atmospheric parameters arise mainly through the choice of the gain matrix and the background information (Ho et al. 2012; Steiner et al. 2013)

At the DMI the a priori background information in use, is the MSIS climatology and the SO is based on an Optimal Linear Combination (OCL) approach by Gorbunov (2002).

It has been discussed in Gobiet and Kirchengast (2004) and also Foelsche et al. (2008) that when using the MSIS climatology as a background climatology in SO, problems will arise at higher latitudes and altitudes. In stratospheric winter conditions temperatures are so low that the MSIS library search finds no adequate profile which fits the cold conditions, and hence, the best fitting profiles are simply too warm. Also Steiner et al. (2013) show that differences between the processing centers increase with altitude and latitude. Furthermore they observe that processing centers which use climatologies, such as, DMI, German Research Centre for Geosciences (GFZ), and University Corporation for Atmospheric Research (UCAR), show larger trends in the atmospheric parameters than the other processing centers.

Based on the problems with the standard retrieval used at the DMI with the MSIS climatology in the SO procedure, and the general discrepancy in results between different processing centers, the average bending angle approach is introduced and tested for CHAMP data. Zonal monthly mean bending angle climatologies are primarily built and secondly, forwarded through the Abel transformation, to obtain zonal monthly refractivity climatologies (Ao et al. 2012; Gleisner and Healy 2013).

Building averages in bending angle space has the advantage that noise is suppressed or at least reduced, and mean bending angle profiles can be used up to higher altitudes. The goal of the study is to circumvent SO in the retrieval of atmospheric parameters, which is detected, as explained, as a major error source between different processing centers. The averaged bending angle CHAMP data is used up to an altitude of 80 km, above that an extrapolation of the averaged bending angle profiles to infinity is still necessary, due to the upper boundary of the Abel integral, see Eq. 3.1. Gleisner and Healy (2013) used an exponential extrapolation with a constant scale height of 7.5 km. The assumption of a constant scale height is connected with the assumption of an unrealistic isotherm atmosphere. Improved extrapolations to infinity could be realized with variable scale heights or with a climate model. However, at stratospheric altitudes the error made with that assumption is already very small and hence negligible. For accuracy the effect of different scale heights was still tested, and is described in Subsection 5.1.3.

Chapter 4 will explain how the bending angle averages are built and Chapter 5 shows the results for the refractivity climatologies, comparing the standard retrieval with SO from the DMI (standard retrieval) and the new average bending angle approach (new retrieval), for CHAMP as well as COSMIC satellite data. Conclusions are drawn in Chapter 6.

4 CHAMP bending angle averages

As a primary investigation, CHAMP bending angle averages are built analog to the COSMIC bending angle averages calculated in Gleisner and Healy (2013), as monthly mean zonal climatologies. The bending angle profiles are interpolated on a 100 m grid as a function of impact altitude. The height dependency impact altitude, H_a, must be changed to impact parameter, a, before computing refractivity profiles from bending angle profiles via an Abel transformation. They are related through

$$a = H_a + R_c + u \ , \tag{4.1}$$

with R_c being the local radius of curvature of the reference ellipsoid and u is the undulation, i.e., the height above the ellipsoid. Since each profile has its own radius of curvature we choose an average radius of curvature within a zonal bin, i.e.,

$$\bar{R}_c = \frac{1}{m} \sum_{i=1}^{m} (R_{c,i} + u_i) \ , \tag{4.2}$$

with m being the number of profiles within a bin.

The bending angle means and medians are then calculated within a month for 10° latitudinal bins. The climatology for the latitudinal bins is calculated by setting up a two-dimensional subgrid structure, and area weighting within each subgrid. For the case of 10° latitudinal bins this results in one subgrid of 2.5° below and one subgrid of 2.5° above the original 10° grid, where each subgrid has a grid width of 5° and once again 18 bins. The mean latitudes for each grid are then:

$$\begin{aligned} \phi_u &= \{-85°, -75°, ..., 85°\} \\ \phi_u^1 &= \{-87.5°, -77.5°, ..., 82.5°\} \\ \phi_u^2 &= \{-82.5°, -72.5°, ..., 87.5°\} \end{aligned} \tag{4.3}$$

with ϕ_u being the original grid structure and $\phi_u^{1,2}$ the two subgrid structures. Respectively we find the following fundamental bins and subgrid bins:

$$\begin{aligned} \text{Original grid} &: [-90° \text{ to } -80°, -80° \text{ to } -70°, ...] \\ \text{Subgrid 1} &: [-90° \text{ to } -85°, -80° \text{ to } -75°, ...] \\ \text{Subgrid 2} &: [-85° \text{ to } -80°, -75° \text{ to } -70°, ...] \end{aligned} \tag{4.4}$$

The area of such a subgrid surface at mean subgrid latitude $\phi_u^{1,2}$ is then calculated by

$$A(\phi_u^{1,2}) = 2\pi r_E^2(\sin(\phi_u^{1,2} + 5/2) - \sin(\phi_u^{1,2} - 5/2)), \tag{4.5}$$

where u reaches from 1 to 18, and r_E is the radius of the Earth. The mean bending angle profile $\alpha(\phi_u)$ for a 10° fundamental bin is obtained by:

$$\alpha(\phi_u) = \frac{A(\phi_u^1) * \alpha(\phi_u^1) + A(\phi_u^2) * \alpha(\phi_u^2)}{A(\phi_u^1) + A(\phi_u^1)}, \tag{4.6}$$

where $\alpha(\phi_u^{1,2})$ is the mean bending angle in a subgrid bin calculated as a simple sum of all bending angles within this bin, weighted by the number of profiles. For simplicity reasons the dependance on altitude has been ignored in Eqs. 4.5 and 4.6.

With Eq. 4.6 we have established how to calculate mean bending angle profiles for fundamental bins. Figure 4.1 shows first results of monthly mean, as well as, monthly median bending angles for CHAMP satellite data and 10° latitudinal bins, for January 2007. Below 50 km, errors resulting from ionospheric residuals, instrumental errors and neutral-atmosphere variability are suppressed due to averaging over many profiles within a bin. Above that, large-scale wiggles appear in the mean bending angle data, leading to sometimes even negative bending angles. The median bending angle profiles do not show such large-scale variations, however small-scale variations clearly appear. The variations can be made even more evident by studying the difference of the bending angle means and medians to the smooth ECMWF analysis data mapped to bending angle space, see Figure 4.2. The large differences to the reference profile exceed for the case of the mean bending angle data sometimes even 4 μrad (l.h.s. of Figure 4.2).

4.1 Bending angle quality control

The DMI uses in the processing from raw data to single bending angle profiles several screening steps in their quality control, in which data is partly or totally rejected (Gorbunov et al. 2006). However, regarding the increased noise in the usage of CHAMP satellite data compared to COSMIC satellite data, I decided to investigate the single bending angle profiles contributing to the monthly mean bending angle estimates of a fundamental bin, more thoroughly.

Figure 4.3 and Figure 4.4 show for each 10° zonal bin all single profiles used in the estimation of the mean bending angle profile. The figures are displayed down to an altitude of 40 km. Clearly, single bending angle profiles with values more than $\pm 50\,\mu$rad contribute to the average values plotted in blue color. The fundamental bins show, dependent on altitude, large standard deviations (green lines), starting to increase sometimes at an altitude of about 50 km (see e.g., Figure 4.3 at mean latitude of 15°). Based

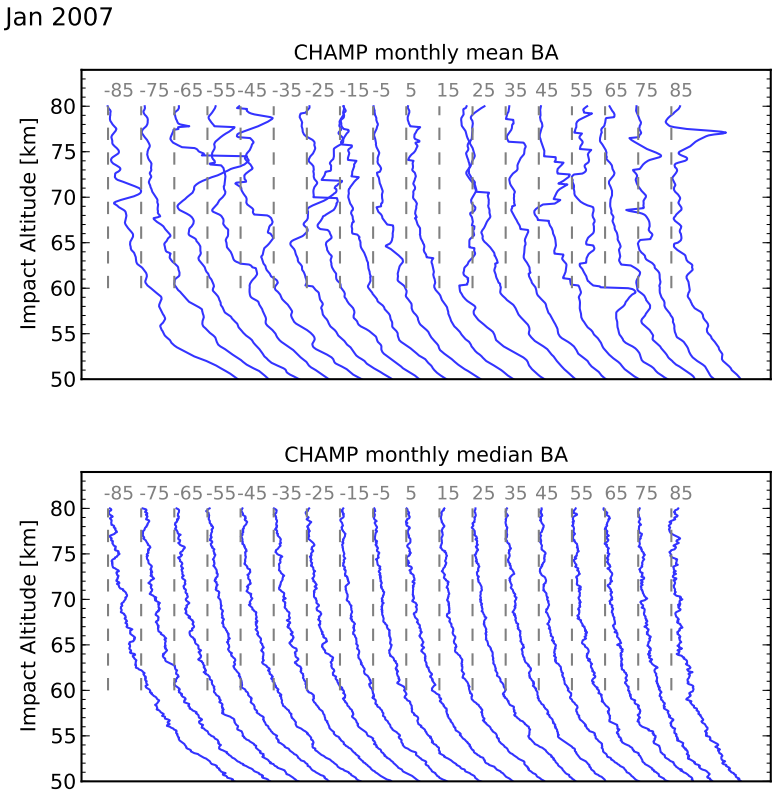

Figure 4.1: Observed bending angle means (top plot) and medians (bottom plot), for CHAMP data from January 2007 and 10° latitudinal bins.

on this analysis, I decided to perform an outlier rejection similar to the discussion in the ROM SAF report by Foelsche and Scherllin-Pirscher (2011). They decided to reject all bending angle profiles to contribute to their climatology which are smaller than $-40\,\mu$rad or larger than $40\,\mu$rad in an altitude region between 50 km and 80 km. In my case, I chose to do an even more strict outlier rejection at an bending angle value of $\pm 30\,\mu$rad in the same altitude region between 50 km and 80 km. Usually we find for the CHAMP satellite, after applying the initial quality control from the DMI, between about 4000 up to 5000 profiles per month. The additional bending angle quality control reduces this number of profiles per month for a value of about 100 up to 600 profiles.

In Figure 4.5 the mean and median bending angle results for CHAMP data from the

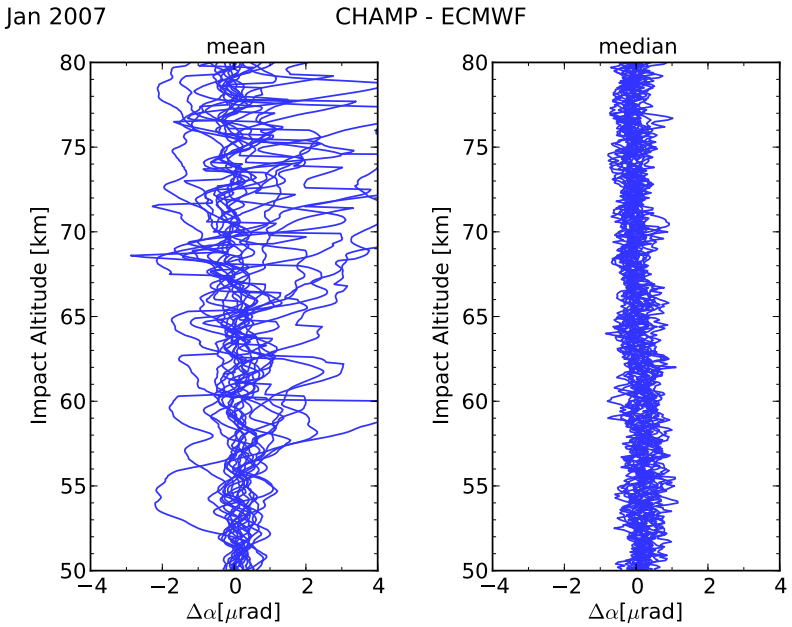

Figure 4.2: On the l.h.s. the difference between observed bending angle means and co-located ECMWF analysis data is plotted, while the r.h.s. shows the difference between bending angle medians and their co-located ECMWF profiles.

same month as in the previous figures, i.e., January 2007, are shown. In contrast to the previous data sets, additional bending angle quality control, i.e., an outlier rejection, has been applied. Clearly, the results for the estimate of the mean bending angle have improved. Rejecting the outliers removes large-scale wiggles in the mean bending angle climatology (top plot), while the median bending angle is almost unaffected by the new approach (bottom plot). Studying also differences to the ECMWF reference profiles confirms, large differences are removed (see Figure 4.6). Finally, I present the results of the single profiles contributing to the fundamental bin in Figure 4.7 and Figure 4.8. The results are encouraging. Profiles with large variations are eliminated and the standard deviations are more a less constant values around the mean values with increasing altitude.

4.2 Combinations of mean and median bending angles

In the article published by Gleisner and Healy (2013), the authors show in their article that observational bending angle data is strongly influenced by large measurement er-

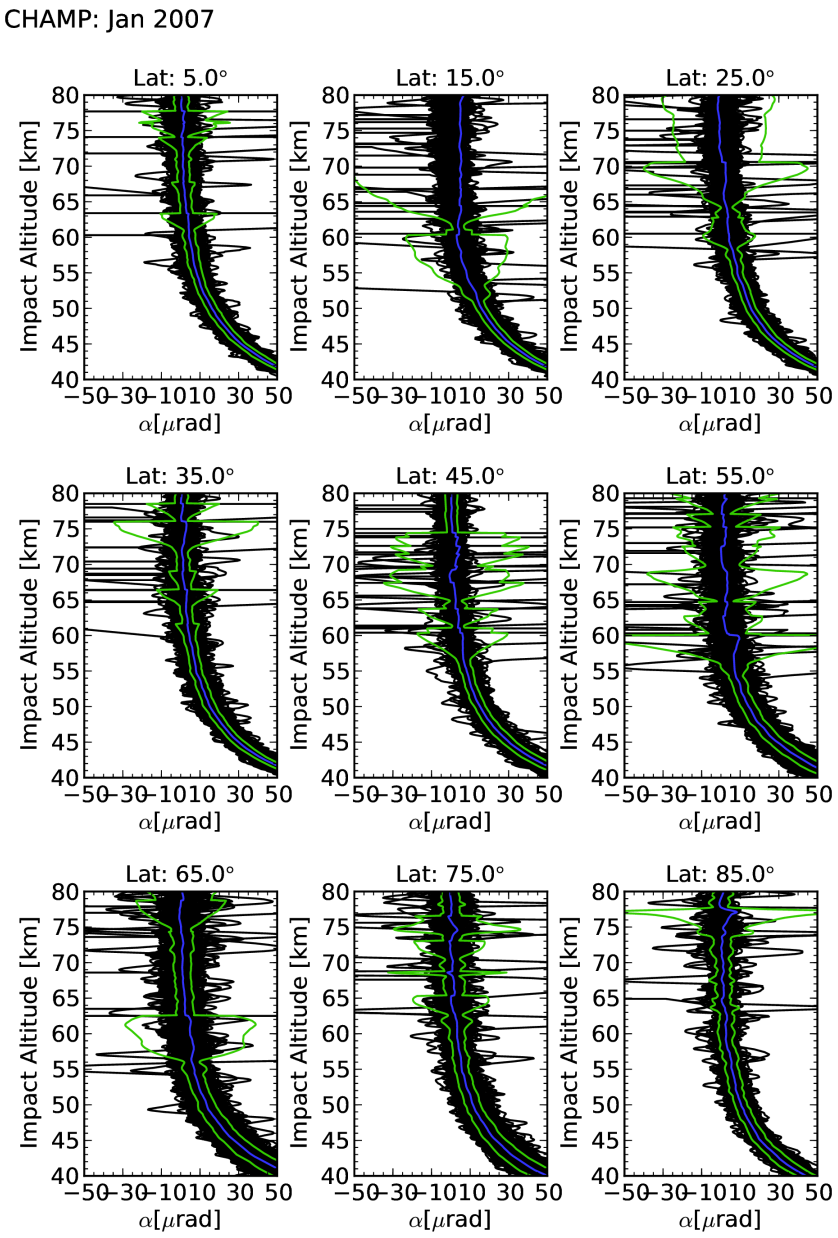

Figure 4.3: The plot shows all observational bending angle profiles for northern fundamental bins. The blue line represents the mean value of all profiles for each bin, the green line its standard deviation.

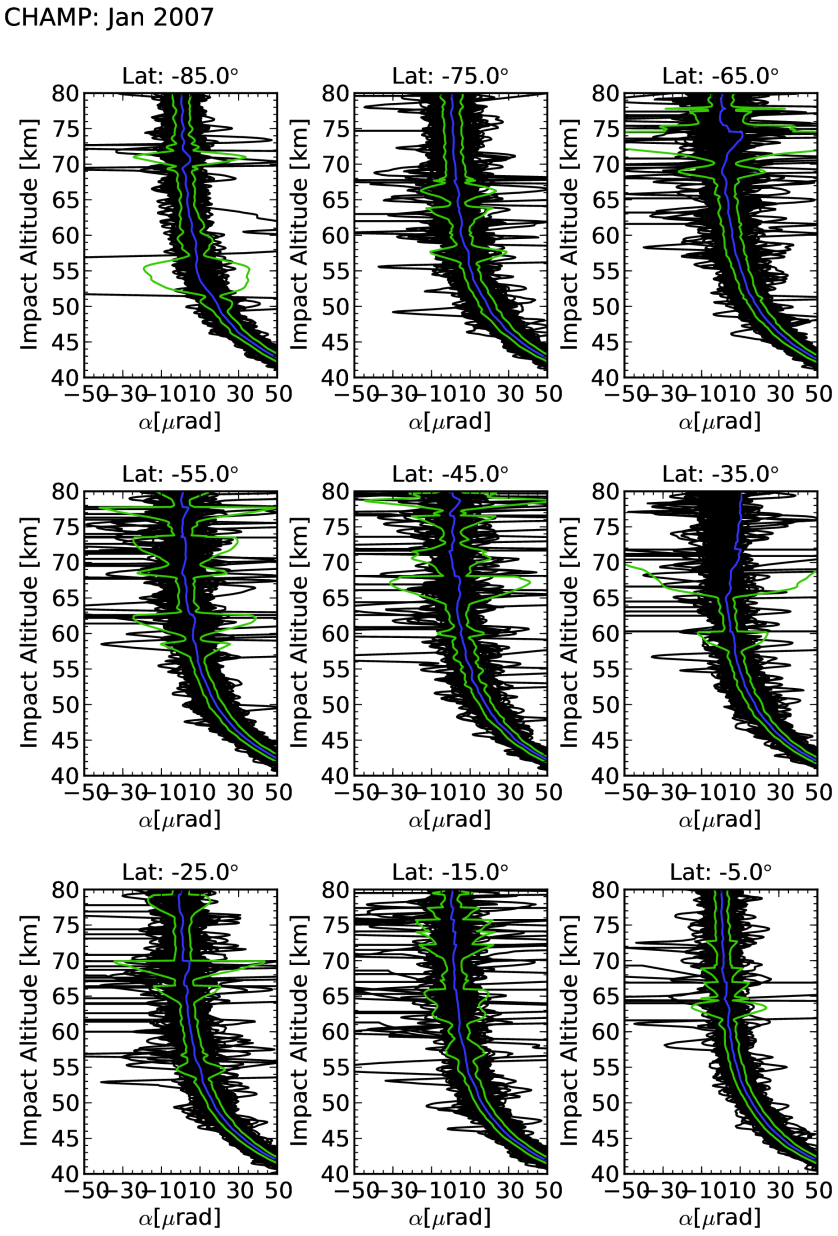

Figure 4.4: The plot shows all observational bending angle profiles for southern fundamental bins. The blue line represents the mean value of all profiles for each bin, the green line its standard deviation.

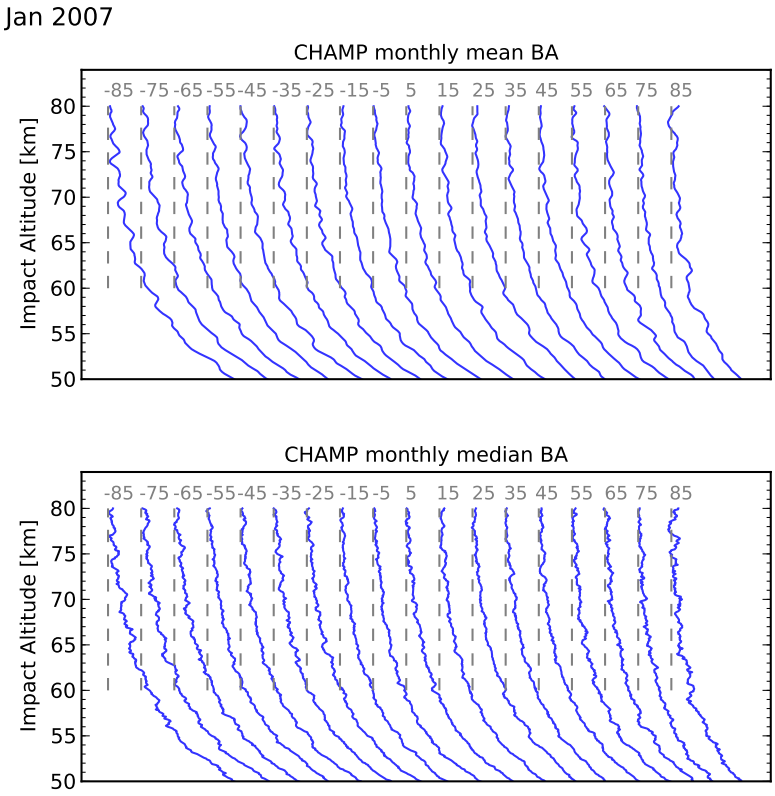

Figure 4.5: Observed bending angle means (top plot) and medians (bottom plot), for CHAMP data from January 2007 and 10° latitudinal bins. Additional quality control has been applied.

rors, as well as ionospheric errors above an altitude of 50 km. Their results have been confirmed by the previous series of plots (Figure 4.1 to Figure 4.4), where without the outlier rejection, large-scale wiggles appear for mean bending angle estimates. They conclude that the mean value is not a robust estimate for neutral-atmospheric bending at higher altitudes, whereas the median value is a much more robust estimate. Therefore Gleisner and Healy decided to use a combination of mean and median value for there bending angle estimate within a month. They used mean bending angles up to an altitude of 50 km. Between the altitude range of 50 km to 60 km they performed a simple linear combination between mean and median, and above 60 km only the median is used for the bending angle estimate. The linear combination, performed to obtain a smooth

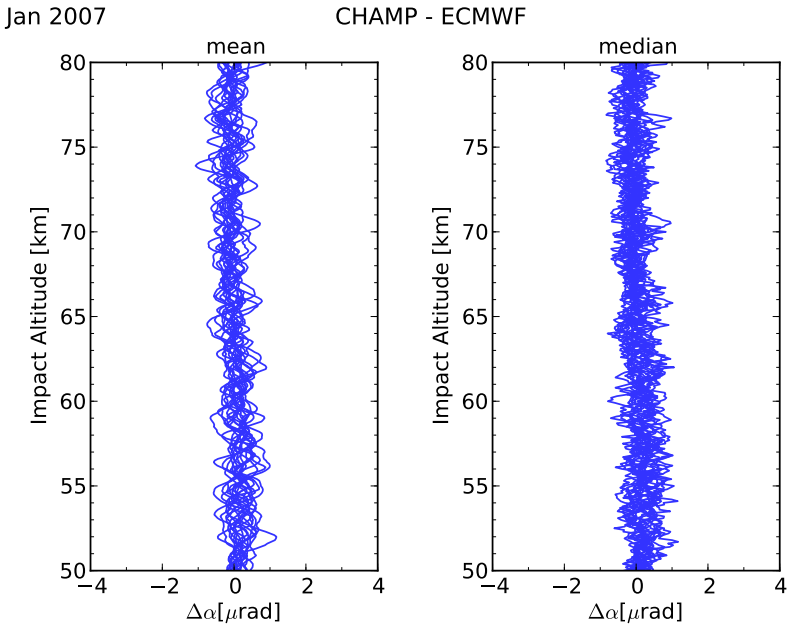

Figure 4.6: On the l.h.s. the difference between observed bending angle means and co-located ECMWF analysis data is plotted, while the r.h.s. shows the difference between bending angle medians and their co-located ECMWF profiles. Additional quality control has been applied.

transition between mean and median is done in the following way:

$$\alpha = (1 - \beta) * \alpha_{\text{mean}} + \beta * \alpha_{\text{median}} \ , \tag{4.7}$$

with β being an increment of 0.01, increasing every height level between 50 km to 60 km for this amount (altogether 100 height levels). Such a bending angle mean-median combination will then be forwarded through the Abel transform, see Eq. 3.1.

Their approach of a mean-median combination is feasible for COSMIC data sets, but regarding CHAMP data it is at least in the same altitude range, questionable. In Figure 4.1 we could observe mean bending angle estimates with sometimes large fluctuations above an altitude of about 50 km. This large-scale fluctuations would have an effect on the bending angle mean-median transition region (50 km to 60 km). This further supports the attempt to perform an outlier rejection on the single profiles contributing to the fundamental bins for CHAMP data. In order to substantiate my argument I show in Figure 4.9 the bending angle difference of mean-median combinations to ECMWF reference profiles. The l.h.s. of Figure 4.9 shows differences where the mean-median combination has been calculated without performing an additional bending angle quality control,

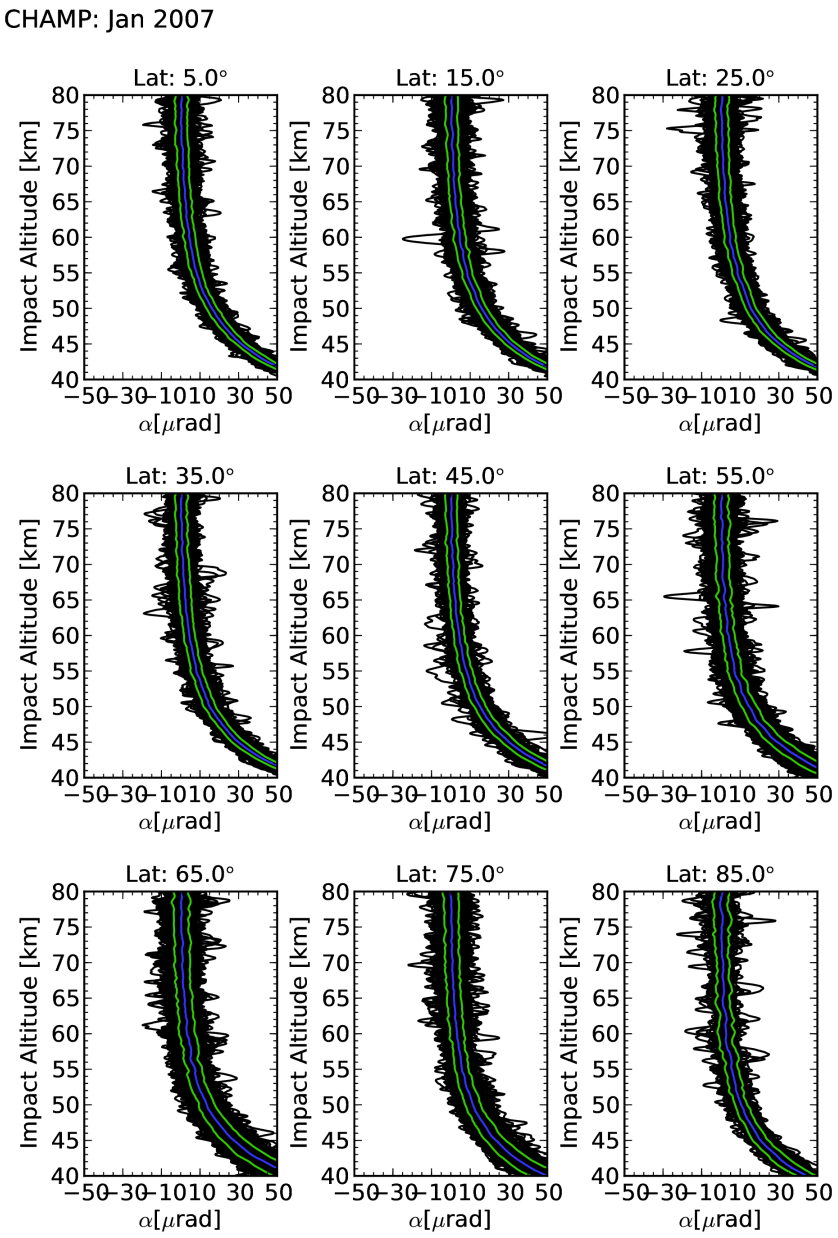

Figure 4.7: The plot shows all observational bending angle profiles for northern fundamental bins. The blue line represents the mean value of all profiles for each bin, the green line its standard deviation. Outliers $\pm 30\,\mu$rad are removed from the single profiles.

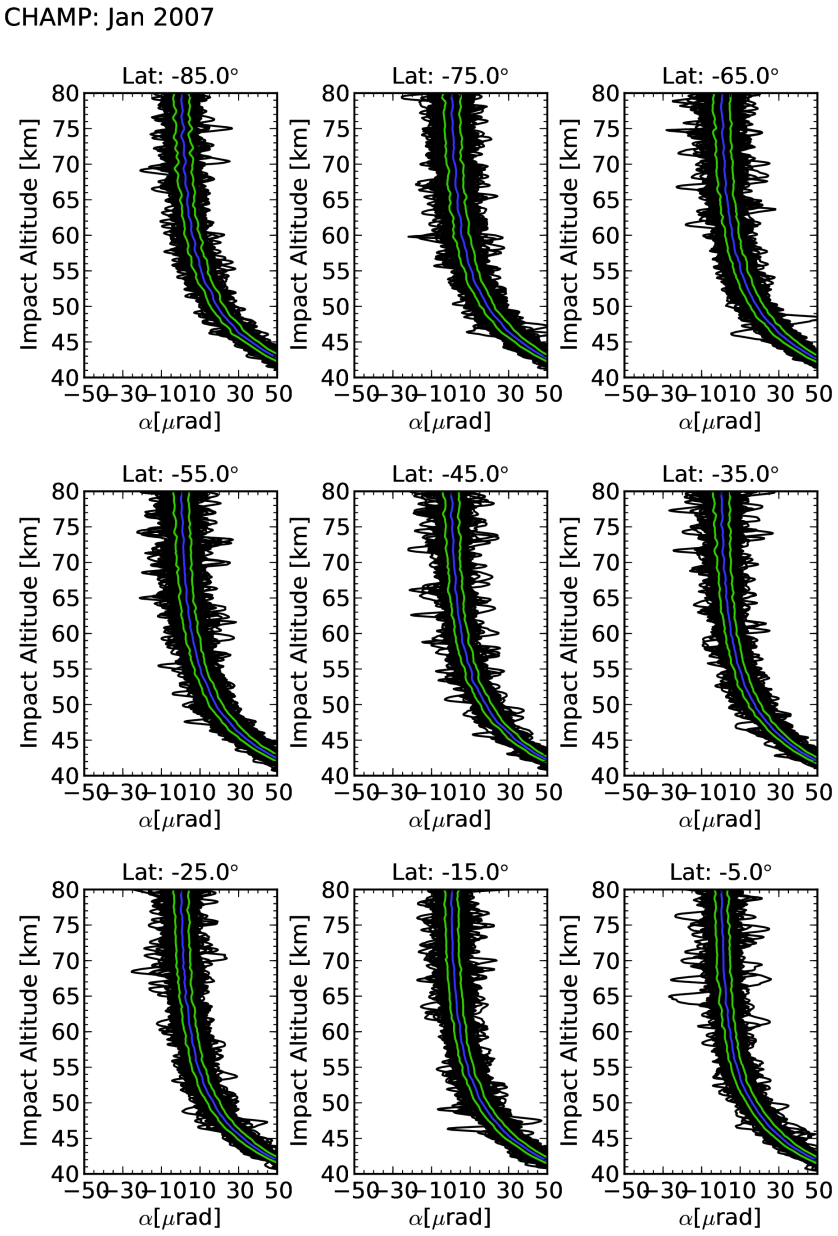

Figure 4.8: The plot shows all observational bending angle profiles for southern fundamental bins. The blue line represents the mean value of all profiles for each bin, the green line its standard deviation. Outliers $\pm 30\,\mu$rad are removed from the single profiles.

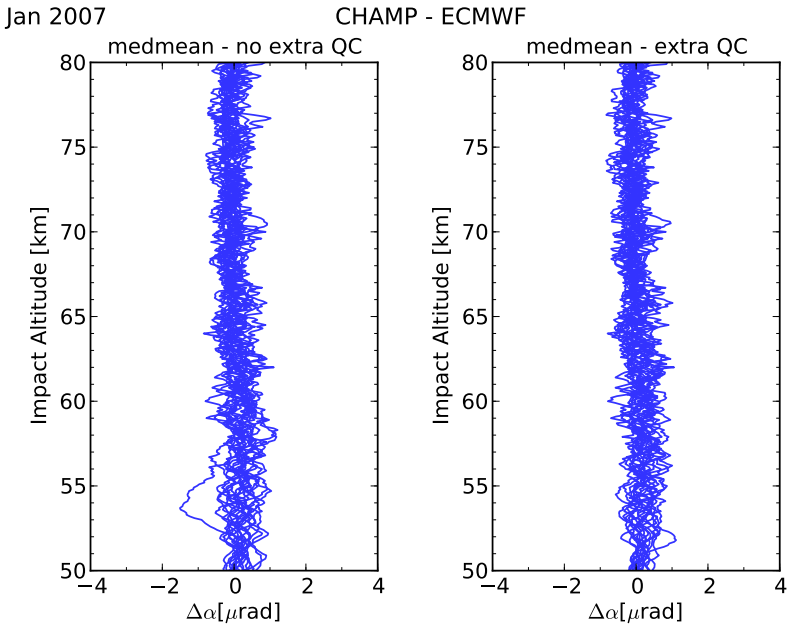

Figure 4.9: The plot illustrates the bending angle difference between the bending angle mean-median combination and its co-located ECMWF analysis profile, for January 2007. On the l.h.s. no outlier removal has been performed before the estimate of the mean-median profile, while on the r.h.s. the results are shown when applying additional quality control.

while on the r.h.s., an outlier rejection has been applied on the bending angle profiles. On the l.h.s. plot we find a single bending angle profile exhibiting a deviation of about $-2\,\mu$rad from the smooth ECMWF reference profile. On the r.h.s. the differences are comparably small, i.e., the bending angle estimates are smoother. Consequently this encourages the idea of applying an additional quality control on the single bending angle profiles before calculating bending angle means.

Finally, different transition heights for the mean-median combination have also been tested. I compared transition heights between 45 km to 55 km, 50 km to 60 km, and 55 km to 65 km, with and without the outlier rejection. Moving the transition height down to 45 km to 55 km reduces the contribution of outliers to the mean-median combination, while raising the transition height naturally increases its contribution. Hence lowering the transition height could be an option for obtaining a better bending angle climatology. On the other hand, it has the negative effect that in regions where measurement errors are not a major error source (below 50 km), in principle the mean value is a much smoother estimate than the median, which suffers from small-scale variations.

Additionally, also between 45 km and 55 km outliers could be part of the mean-median bending angle estimate. As a consequence, I first decided to always apply an additional quality control on the single bending angle profiles to improve the mean bending angle estimate and second, run a mean-median combination through the Abel transform with a transition height between 50 km and 60 km. However, I analyzed the effect of different transition heights on the refractivity climatology when applying first the outlier rejection. The influence of the choice of the transition height is minimal and will be discussed in Subsection 5.1.2.

5 Refractivity Results

Zonal monthly mean refractivity profiles are computed for CHAMP data as well as COSMIC data, using the new average bending angle approach as well as the standard single profile processing. Section 5.1 will discuss consequences of different bending angle averaging methods on refractivity climatologies. Having established a suitable averaging method of monthly zonal bending angle means, an initial analysis of zonal mean refractivity profiles is given in Section 5.2. Afterwards, a systematic comparison between the new retrieval and the standard retrieval is given in Subsection 5.3.1. And finally, Subsection 5.3.2 discusses differences between CHAMP and COSMIC data, using the two inversion methods.

5.1 Implication of different bending angle averages on refractivity

Two different approaches of calculating bending angle averages have been discussed in the previous section. First, the possibility of applying an additional bending angle quality control on the single profiles (Section 4.1), and second, the possibility of different mean-median height combinations (Section 4.2). The effect of this different approaches on the monthly refractivity profiles will be assessed in this section. Furthermore, the consequence of setting a fixed scale height in the exponential extrapolation for the Abel transformation is also tested and discussed.

5.1.1 Impact of quality control

As a primary investigation I want to know how large the effect of applying an additional bending angle quality control (QC) is on monthly mean refractivity profiles. To answer this question, monthly mean refractivity profiles have been calculated with and without additional QC. Figure 5.1 shows the relative difference between monthly mean refractivities obtained by average-profile inversion, calculated with "Old QC" and with "New QC", for CHAMP data from January 2007. "Old QC" refers to the standard QC at the DMI, applied on single profiles (Gorbunov et al. 2006), "New QC" refers to an additional outlier rejection at bending angle level. Differences larger or smaller $\pm 1.2\%$ are not color-coded, since I want to focus on the main range of values. For January 2007

largest differences are found between 60 °N to 90 °N, starting at an altitude of about 20 km, resulting in a relative difference of about 0.5% at 40 km altitude, reaching about 1% at 47 km altitude. Between 90 °S to 80 °S January also exhibits differences, starting at an altitude of about 35 km, increasing with altitude to more than −1%. In July a similar refractivity difference, switched to southern latitudes, can be observed. At 60 °S and 40 km altitude it is again about 0.5%, at 30 °N July shows an additional region of increasing refractivity difference of more than 1.2% at an altitude of 40 km. April shows mainly negative relative differences, starting at an altitude of about 40 km, increasing to sometimes more than −1.2%, and October shows mainly positive differences with values up to about 0.5%.

In Figure 5.2 and Figure 5.3 the relative differences between monthly mean refractivities from CHAMP data and from co-located ECMWF data is shown, calculated with additional QC (bottom panel) and without additional QC (top panel), for January and July 2007. For January the plotted color range is between ±3%, for July between ±5%, since in the latter case the refractivity differences are enhanced. In principle the bottom panel and top panel of each plot are almost identical. For January, the differences to ECMWF are mainly in the range of 0.5% up to 1.5% with a dominant sector between 20 °N to 70 °N latitude, in the height range between 35 km to 50 km altitude. July shows major differences of up to 5%, starting at an altitude of about 40 km in the latitude sector between 90 °S to 50 °S. Since the focus of interest lies in the impact of the additional quality control on the mean refractivity profiles, we compare "Old QC" (top) with "New QC" (bottom). Although the bottom panel and the top panel are very similar, we find exactly in the regions where we know differences between the quality controls exist (see Figure 5.1), a slight improvement towards ECMWF for "New QC". In Figure 5.2 at 60 °N latitude the relative difference is reduced from about 0.5% ("Old QC") to about 0.3% ("New QC"), and respectively in Figure 5.3, at 45 km altitude and 20 °N to 30 °N, a reduction from about 5% to about 1.5% can be observed.

Since the objective is to find a smooth monthly mean bending angle estimate, which can be forwarded through the Abel transform to calculate monthly mean refractivities, the approach to use additional QC is favorable. The effect on refractivity profiles has been illustrated in Figure 5.1, and improvements towards ECMWF have been shown in Figure 5.2 and Figure 5.3. Based on the previous refractivity analysis, as well as, the bending angle analysis in Section 4.1, additional QC will always be applied on the bending angle profiles.

5.1.2 Impact of different mean-median height combinations

Zonal monthly mean refractivities are calculated using the average profile inversion approach with additional bending angle QC. The monthly mean bending angle profiles are

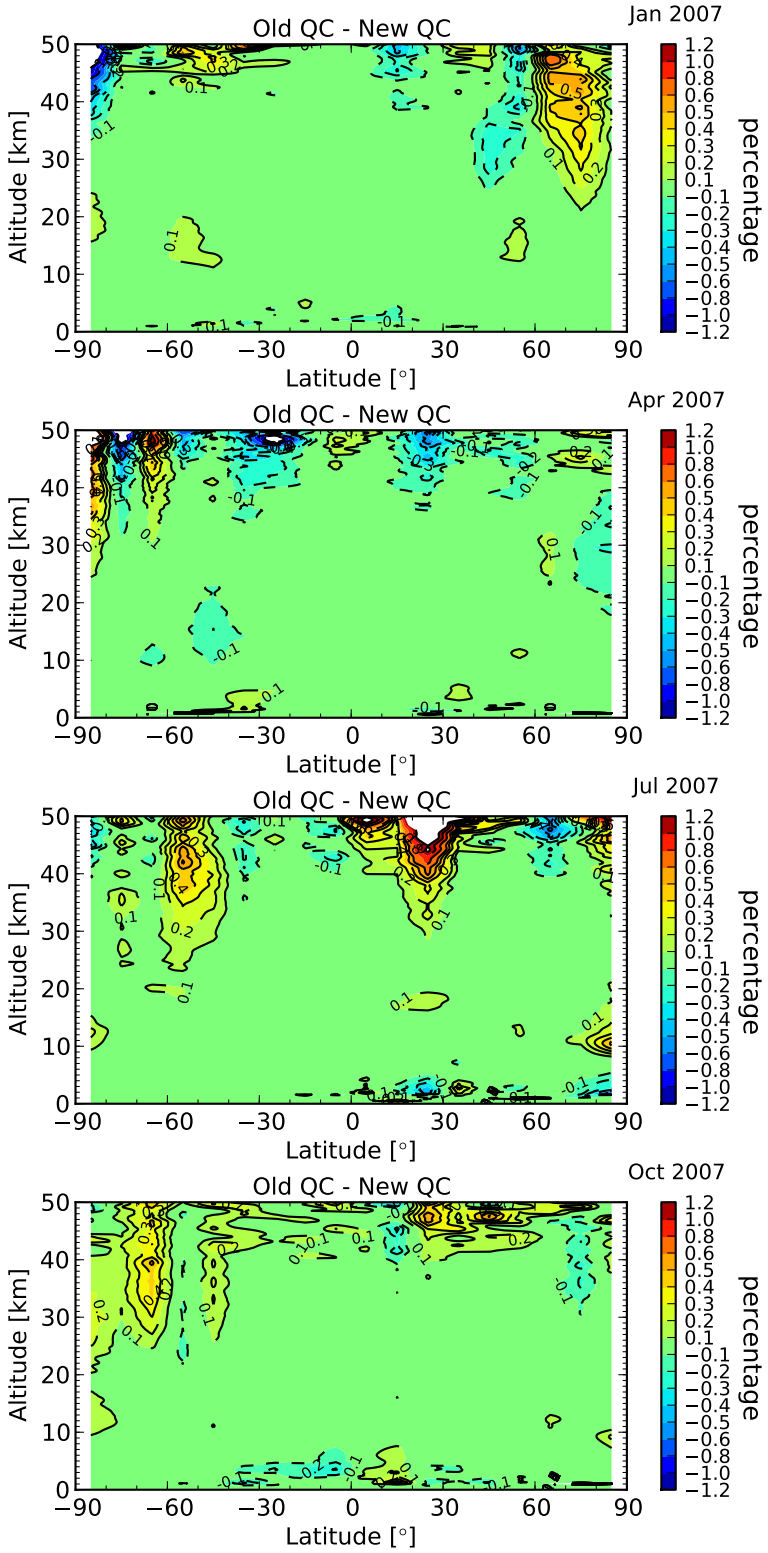

Figure 5.1: Relative difference between monthly mean refractivities obtained by average-profile inversion with standard quality control (Old QC) and additional quality control (New QC), for CHAMP data from January, April, July and October 2007 (from top to bottom).

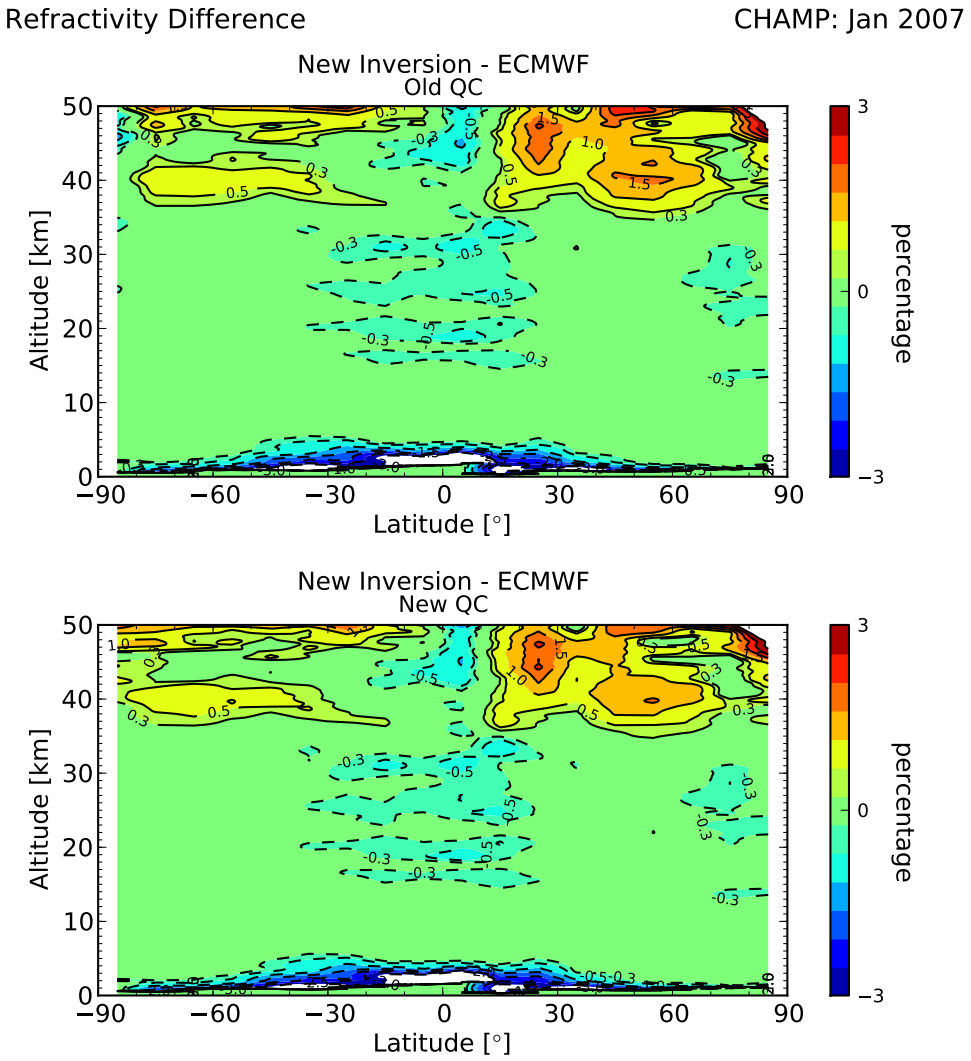

Figure 5.2: Relative differences between monthly mean refractivity from CHAMP data and from collocated ECMWF data, using average-profile inversion with standard quality control (Old QC, upper panel) and additional quality control (New QC, lower panel), for January 2007.

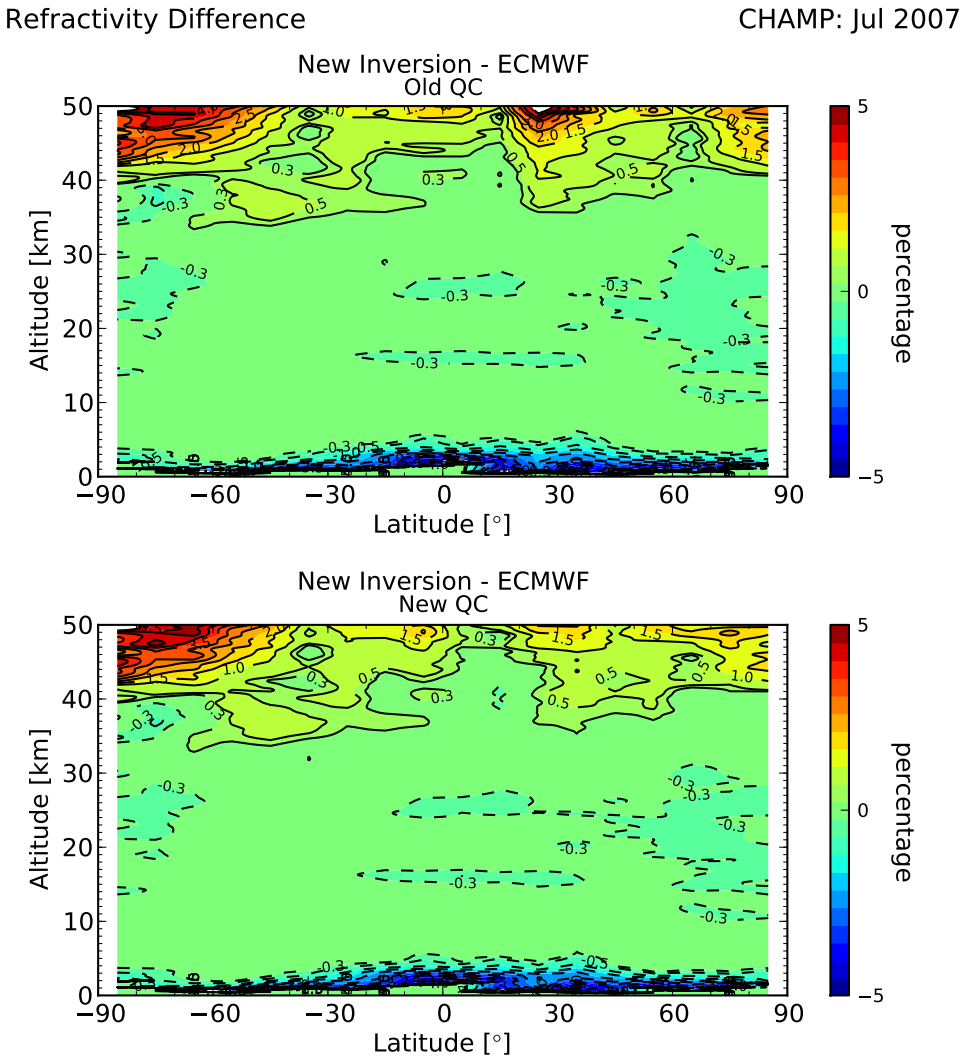

Figure 5.3: Relative differences between monthly mean refractivity from CHAMP data and from collocated ECMWF data, using average-profile inversion with standard quality control (Old QC, upper panel) and additional quality control (New QC, lower panel), for July 2007.

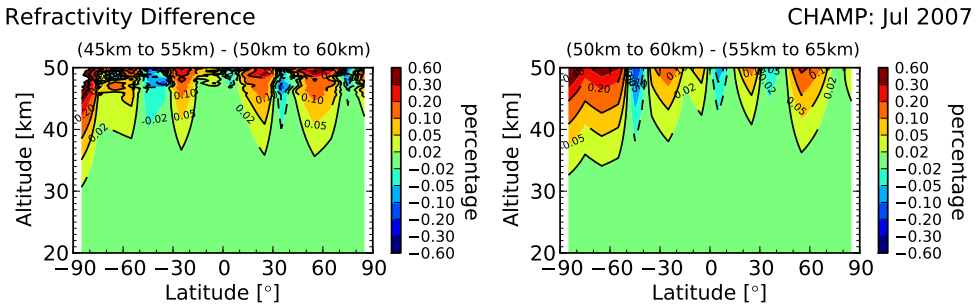

Figure 5.4: Relative difference between monthly mean refractivities obtained by average-profile inversion with additional quality control, calculated for different mean-median height realizations, for July 2007. The l.h.s. compares the transition regions 45 km to 55 km with 50 km to 60 km, the r.h.s. compares 50 km to 60 km with 55 km to 65 km.

built as a combination between a mean bending angle profile and a median bending angle profile, using a region of transition in order to obtain a smooth bending angle (see Eq. 4.7). The effect of different transition heights, on the monthly mean refractivity profiles, is tested in this section. I studied transition regions between 45 km to 55 km, 50 km to 60 km, and 55 km to 65 km. Figure 5.4 shows the relative refractivity difference between a monthly mean refractivity profile, calculated with different transition regions, as a function of latitude and altitude, for CHAMP data and the month July 2007. The l.h.s. compares the lowest transition region with the middle transition region, while on the r.h.s. the middle and the highest transition regions are compared. For both sides of the plot the relative differences are small, starting at an altitude of about 35 km with 0.02%, which is negligible, increasing at an altitude of 50 km, to a value of about 0.3% to 0.6%. I conclude, the choice of the mean-median transition region in the overall tested height range between 45 km to 65 km contributes about one half of one percent to the refractivity, at an altitude of 50 km. Hence, I decided to choose, equally to the COSMIC data sets tested by Gleisner and Healy (2013), a transition region of 50 km to 60 km for the mean-median bending angle combination. Furthermore I repeat the argument given in Section 4.2. The mean value is at least at lower altitudes a more smooth estimate than the median value, which suffers from small-scale variations, whereas at high altitudes the median value provides a robuster estimate. Hence, the optimal choice uses a combination between them, where the smoother mean value is used as high as possible, before the noise increases and large-scale variations prevail.

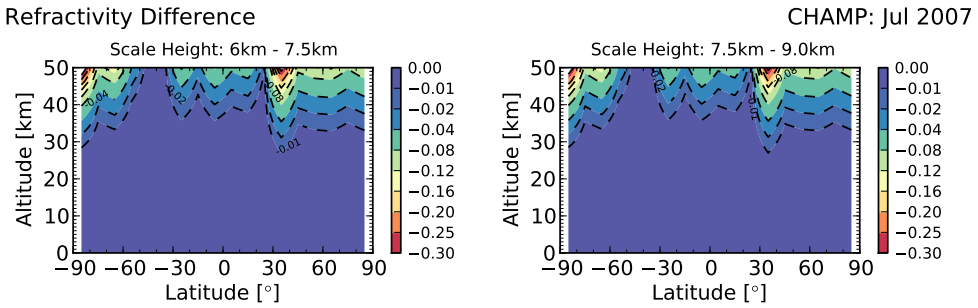

Figure 5.5: Relative difference between monthly mean refractivities obtained by average-profile inversion with additional quality control, calculated for three different constant scale heights, for July 2007. The l.h.s. compares the scale heights 6 km and 7.5 km, the r.h.s. compares 7.5 km and 9 km.

5.1.3 Testing different scale heights

The observed monthly mean bending angle estimates are obtained using mean bending angles up to 50 km altitude, between 50 km to 60 km a mean-median transition region, and above 60 km up to 80 km altitude we use the median value. Above 80 km altitude the observed bending angles have been exponential extrapolated, using a fixed scale of 7.5 km. Since a fixed scale height is only a realistic assumption for an isotherm atmosphere, we test the implication of this assumption. We simulated bending angle continuations as exponential fall-offs with three different constant scale heights, i.e., 6 km, 7.5 km, and 9 km, and analyzed its impact on refractivity.

Figure 5.5 shows the refractivity difference between refractivities calculated at different scale heights, for the month July, using CHAMP data. The left panel compares the results for the scale heights 6 km and 7.5 km, the right panel compares the scale heights 7.5 km and 9 km. The analysis shows that using different scale heights has a negligible impact on the refractivity profiles below 40 km altitude. The l.h.s. and r.h.s. of Figure 5.5 reveal a contribution of only 0.04% to the refractivity at 40 km altitude, increasing to about 0.3% at 50 km altitude. Hence, the errors made in the assumption of an exponential extrapolation with a constant scale height are small in the stratosphere.

With that previous analysis, I close this section which addressed different possible average bending angle realizations. In all future results I apply an additional outlier rejection on the single bending angle profiles. Furthermore I use a mean-median combination for the bending angle estimate with a transition height between 50 km to 60 km, and a fixed scale height of 7.5 km.

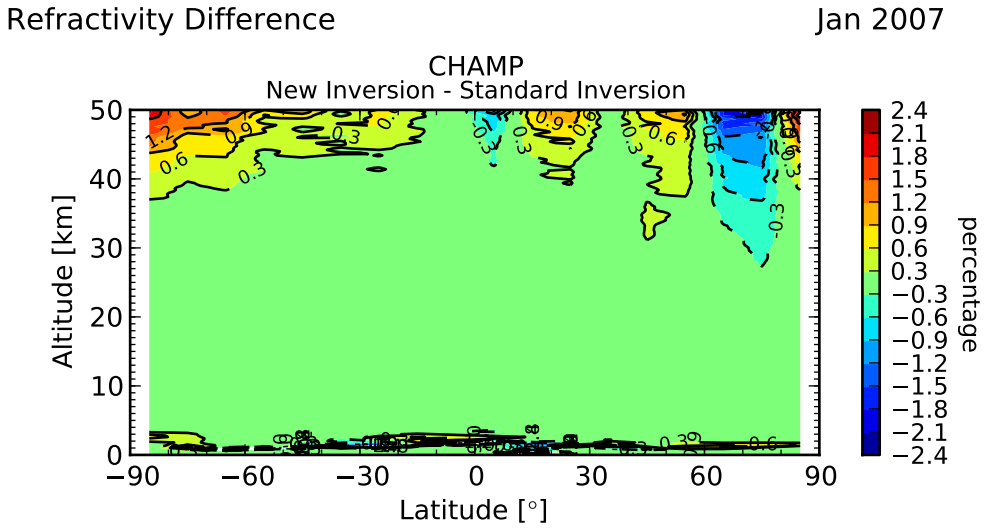

Figure 5.6: Relative difference between monthly mean refractivity from CHAMP data, using average-profile inversion and standard inversion, for January 2007.

5.2 Initial analysis of the average bending angle approach

For January 2007 I show first CHAMP data results of 10° monthly mean refractivity profiles, calculated with the average bending angle approach. As a comparison, the same month was computed using the standard single profile processing. Furthermore the corresponding co-located monthly mean ECMWF analysis data profile was generated. Additionally, the same set (average bending angle approach, standard approach) was computed with COSMIC satellite data, binned also into 10° fundamental bins.

In Figure 5.6 the relative difference between the two inversion methods, i.e., average profile processing and single profile processing, is studied. At an altitude of about 35 km the difference is for January 2007 of the order of ±0.3%, increasing to about more than ±1% at 50 km altitude.

Knowing the regions where main differences between the two schemes occur (see Figure 5.6), it is possible to study its impact on the mean profiles by analyzing the relative difference of each processing method to the co-located monthly mean ECMWF analysis data profile, which is shown in Figure 5.7. The top panel shows the refractivity difference when using the average bending angle approach, the bottom panel shows the difference when using single profile processing. The two panels are almost identical below 35 km, which is encouraging for both inversion methods. Above 35 km the differences towards

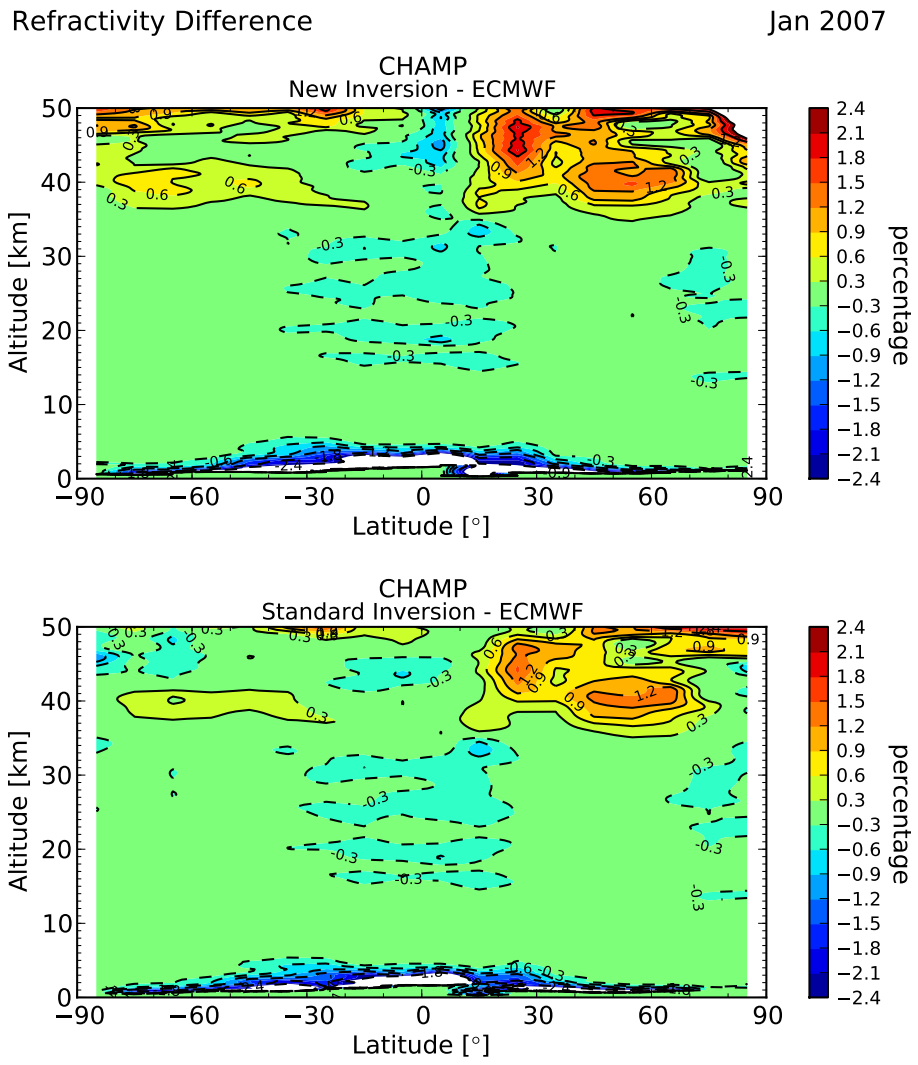

Figure 5.7: Relative difference between monthly mean refractivity from CHAMP data and from collocated ECMWF data, using average-profile inversion (top plot) and standard inversion (bottom plot), for January 2007.

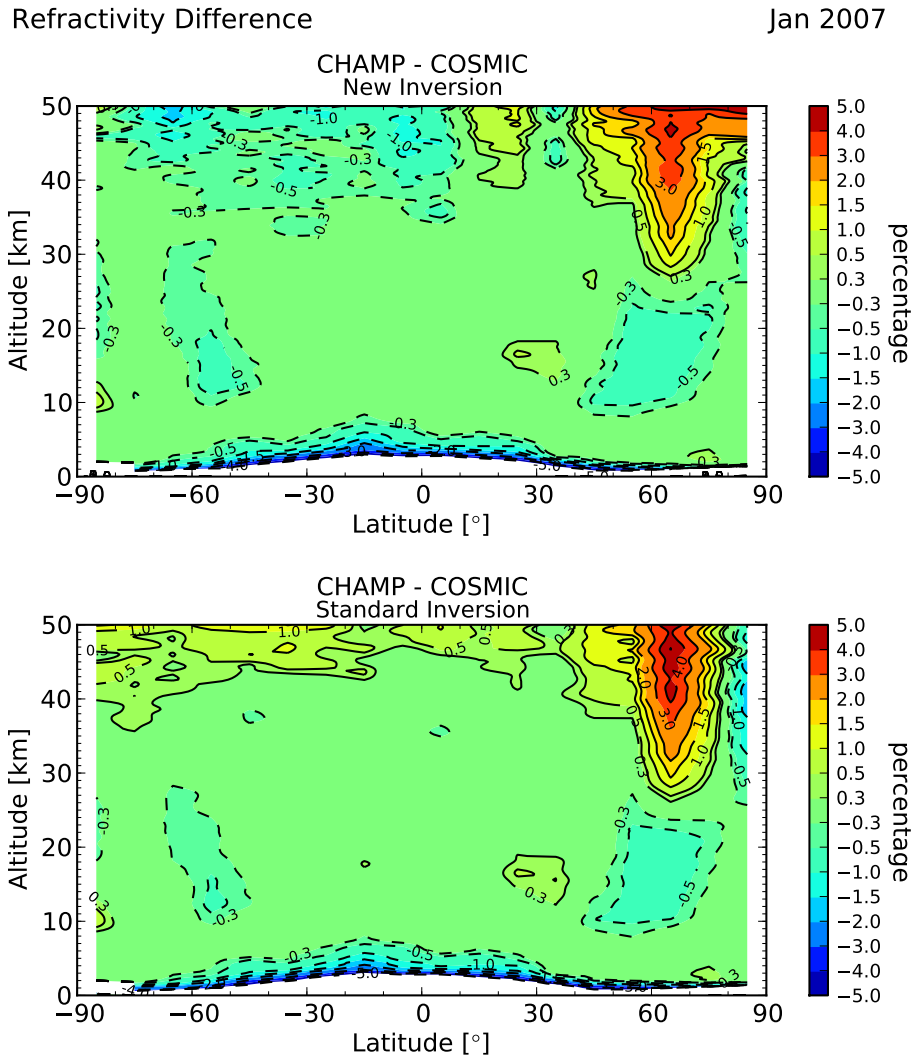

Figure 5.8: Relative difference between monthly mean refractivity calculated with CHAMP data and COSMIC data, using average-profile inversion, for January 2007.

ECMWF increase to up to more than 2%, depending on latitude and altitude. In principle, the two inversion methods show a similar, but not equal pattern in their differences from ECMWF. A detailed comparison of the two processing methods, studied on a longer time scale, will be given in Subsection 5.3.1. Based on one month a conclusion will not be drawn about which method is to favor. So far I only conclude that the average bending approach is also feasible with CHAMP data, and not working exclusively for COSMIC satellite data.

Finally, I am studying in Figure 5.8 the relative difference between CHAMP and COSMIC data sets, processed with the average bending angle approach (top panel), and the single profile processing approach (bottom panel). Once again, below 35 km the two processing methods show a very similar pattern, when comparing different data sets. Above 35 km and at the respective winter polar regions an area appears, with differences of up to 5%, for both processing methods. The remaining latitudes reveal at altitudes between 40 km and 50 km smaller differences of about ±0.5%, with a negative sign for the new and a positive sign for the standard retrieval.

This initial analysis gives a first positive impression about applying the average bending angle approach on CHAMP data. Studied on the basis of one month, I see no major differences in the quality of the refractivity results between the two inversion methods, however emphasizing the clear advantage of the new approach being much simpler than the rather complex implementation of SO. Nevertheless, a much more detailed study, performed in the following section, is necessary.

5.3 Detailed analysis of the average bending angle approach

5.3.1 Comparison of new inversion to standard inversion

One of the motivations for the introduction of the new retrieval scheme is to circumvent the rather complex SO, and hence remove a source of structural uncertainty from the processing. However, we first need to find out if the new retrieval scheme is equally good, or maybe even better, than the standard retrieval scheme. Hence, both processing methods need to be compared and studied on a longer time scale. In order to get a first impression of the performance of the two retrieval schemes, Figure 5.9 plots the relative differences between monthly mean refractivities from CHAMP data and ECMWF data, studying the four months January, April, July and October 2007, comparing new inversion (top row) to standard inversion (bottom row). The plot gives an impression about the seasonal variation of the two schemes for the year 2007, dependent on altitude and latitude. Below 35 km the two methods give very similar results. Also between 35 km and 50 km altitude the relative differences show a similar pattern. The differences are within the range of 6% relative to ECMWF, and vary slightly between the two meth-

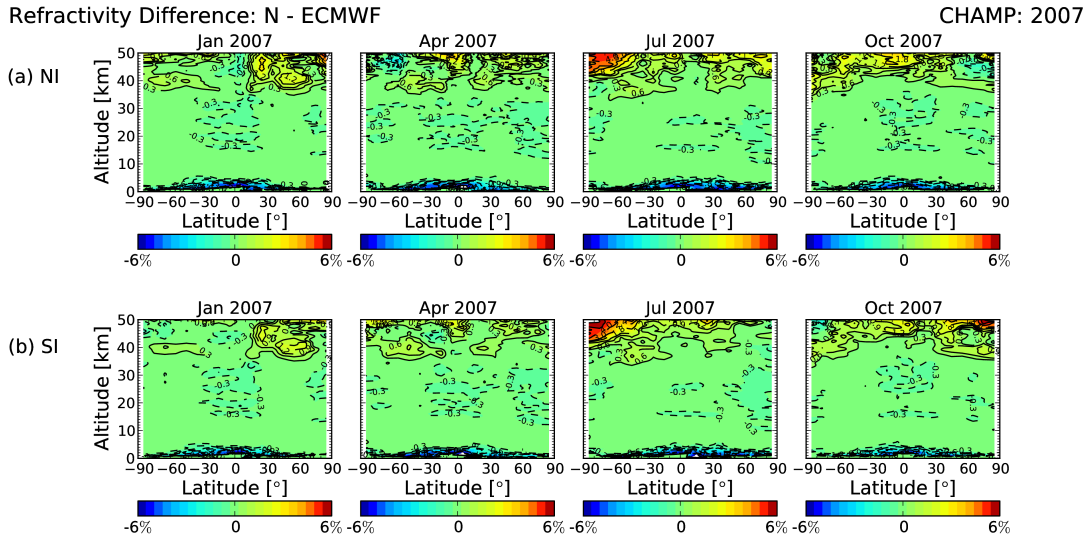

Figure 5.9: Relative difference between monthly mean refractivities from CHAMP data and from collocated ECMWF data, using (a) new inversion (NI, top row) and (b) standard inversion (SI, bottom row), for the months January, April, July and October 2007.

ods. It seems that the main differences are found at higher latitudes, and especially in winter conditions. As mentioned before, the ROM SAF processing facility uses the MSIS climatology as a priori information in their SO, which is known to introduce problems at higher altitudes and latitudes and winter conditions. Circumventing the SO step by using the average bending angle approach leads to the reasonable assumption of main differences between the two methods exactly in that area and season. There is the hope of data quality improvements at high altitude winter polar conditions when using the new retrieval scheme for the investigation of climatologies. For the analysis of individual profiles, the standard approach using SO, is still a requirement. The choice of a good background information for noisy bending angles is of high importance. The DMI has plans to improve their standard procedure by employing the BAROCLIM spectral model, which is expected to improve the quality of the data.

To analyze if the average bending angle approach improves data quality at high latitudes and altitudes, I studied the relative differences between CHAMP and ECMWF data, comparing the two processing methods for higher latitudes and the time period from September 2001 until September 2008. Figure 5.10 and Figure 5.11 show the relative differences for the four higher latitude bands: 80°N to 90°N, 70°N to 80°N, 90°S to 80°S and 80°S to 70°S, for new and standard retrieval (at the blank areas was no data available). The results are very illustrative, since the plots clearly mark as expected for the standard retrieval maximal deviations from ECMWF, for northern or southern winter conditions. The standard retrieval shows a very distinct signal, occurring at polar winter conditions, increasing with altitude and latitude. Furthermore the differences are stronger enhanced on the southern hemisphere, since the Antarctic shows coldest temperatures. Also the new retrieval exhibits a maximum increase of the relative differences in the winter months, but it is slightly reduced compared to the standard retrieval and less distinct. Furthermore an increase of the bias for the remaining non-winter months can be observed. Summarized, analyzing relative differences towards ECMWF and restricting to winter months, the new retrieval shows smaller relative differences compared to the standard retrieval. However, studying the rest of the months of the year the differences slightly increase for the new retrieval.

Finally, in Figure 5.12 differences between RO satellite data and ECMWF analysis data at mid latitudes down to low latitudes are studied for the two processing methods. The left column shows the differences using the new retrieval scheme, the right column the differences using the standard retrieval scheme, studying northern 10° latitude bins in 20° steps. Personally, I think the results are very interesting because obviously the two processing schemes show very similar differences from ECMWF. Only for the highest latitude bin, 60°N to 70°N, the standard retrieval still shows a slightly more enhanced difference in the winter months. With decreasing latitudes towards the equator the results become practically the same. In 2006 there is a change of the seasonal oscilatting

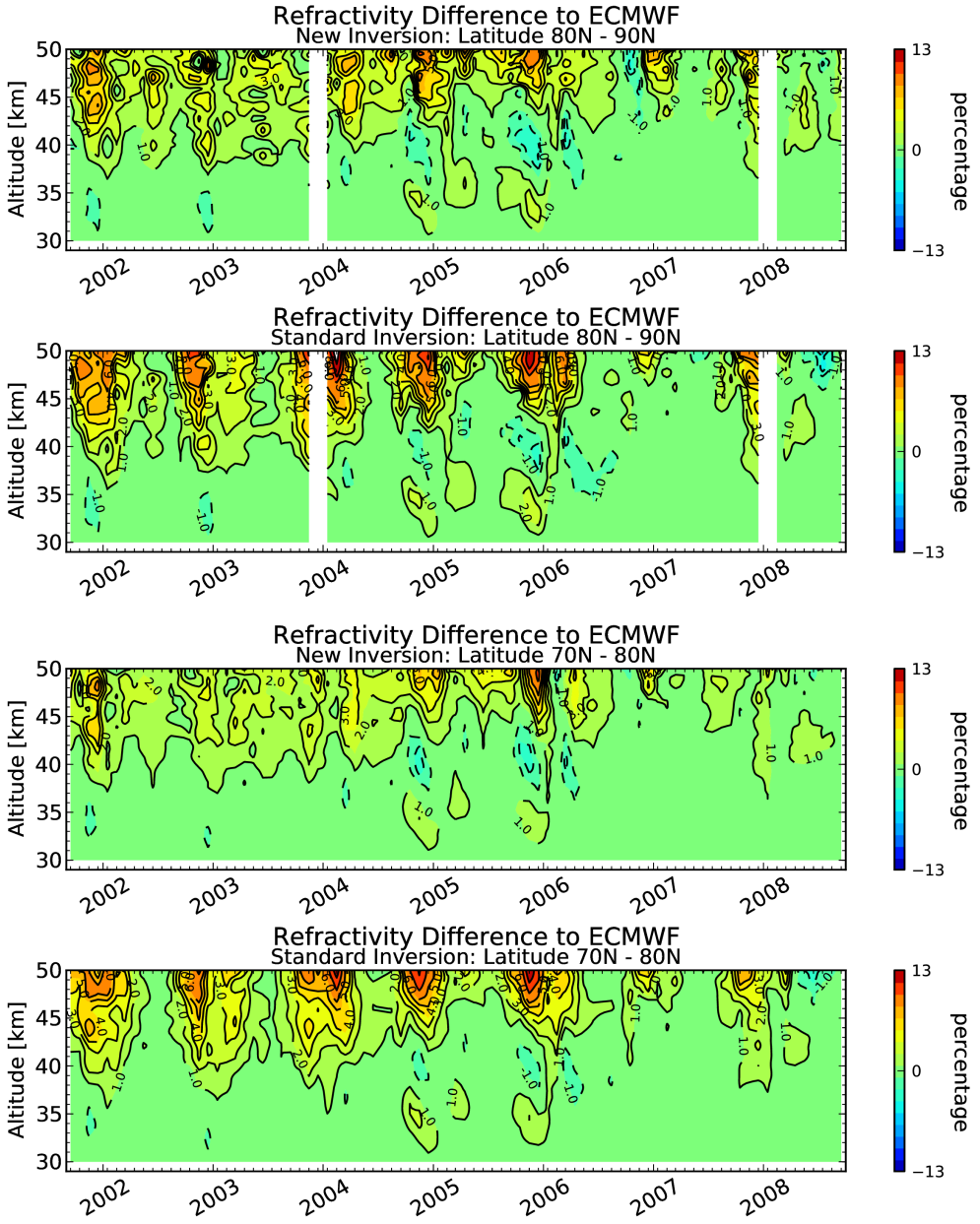

Figure 5.10: Relative differences between monthly mean refractivities from CHAMP data and from collocated ECMWF data, comparing new inversion and standard inversion, from September 2001 until September 2008 for the zonal bins 80°N to 90°N and 70°N to 80°N.

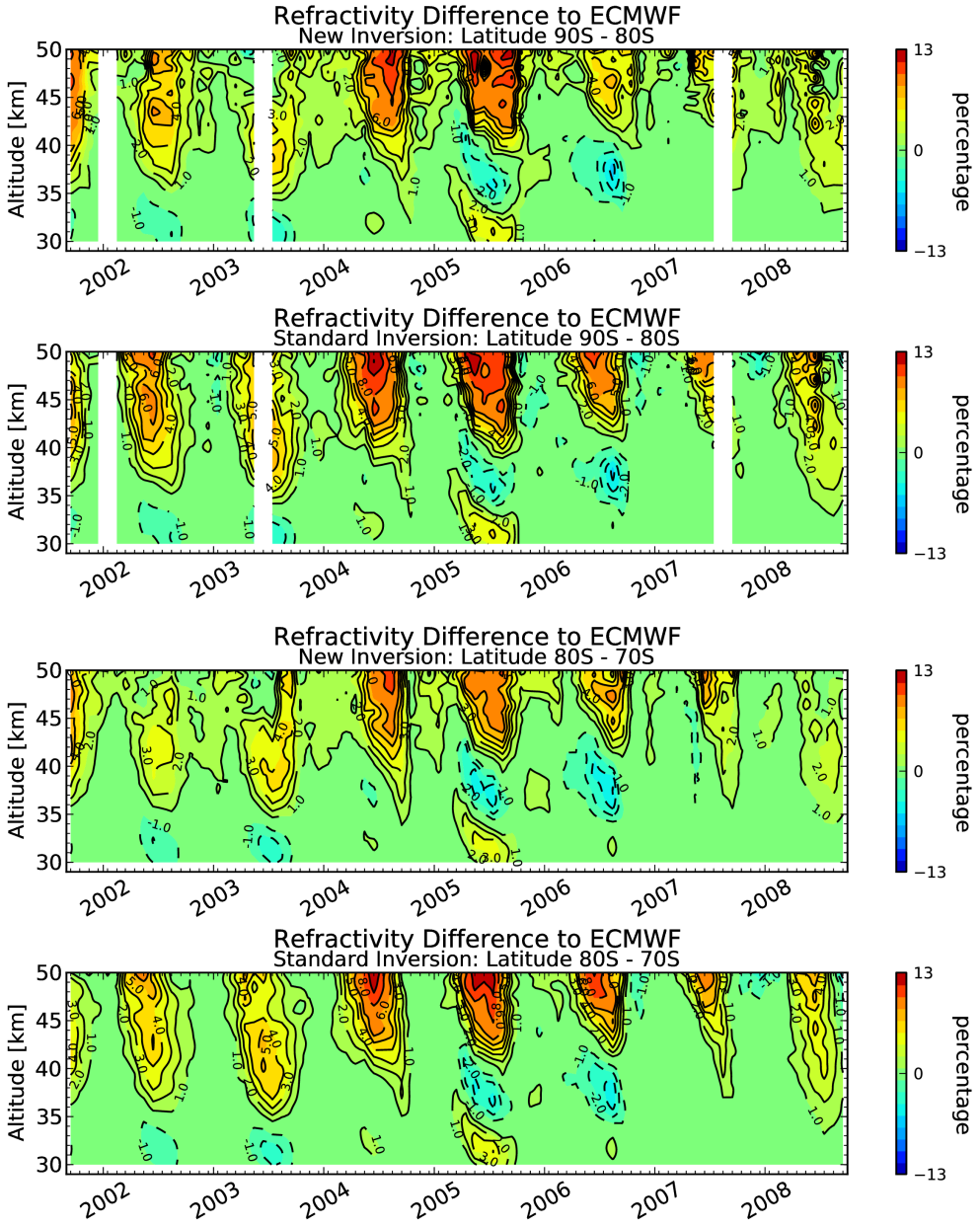

Figure 5.11: Relative differences between monthly mean refractivities from CHAMP data and from collocated ECMWF data, comparing new inversion and standard inversion, from September 2001 until September 2008 for the zonal bins 90°S to 80°S and 80°S to 70°S.

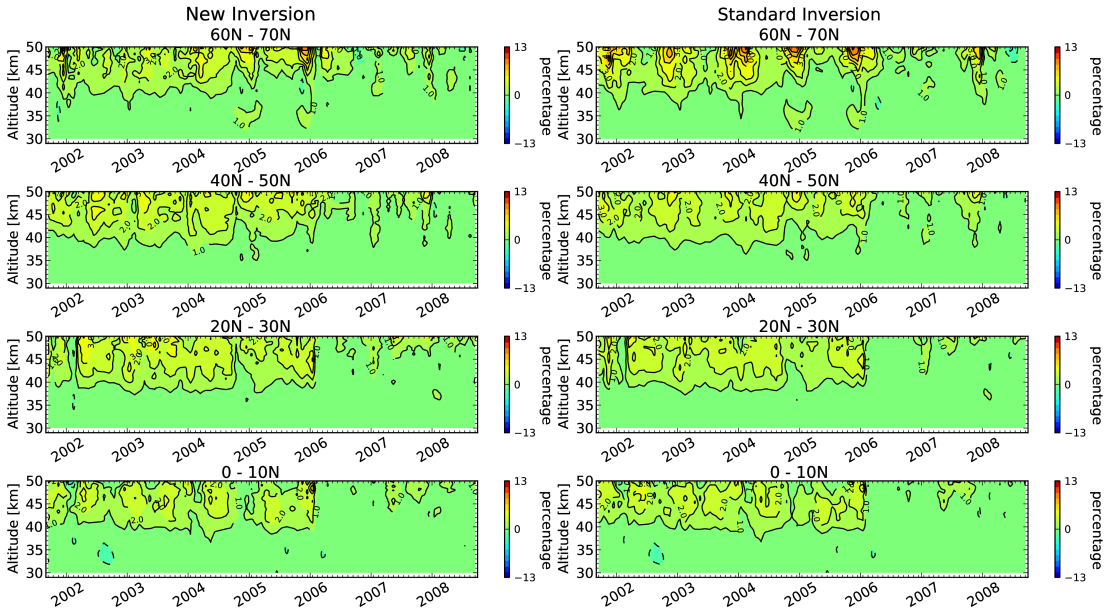

Figure 5.12: Relative differences between monthly mean refractivities from CHAMP data and from collocated ECMWF data, comparing new inversion (l.h.s.) and standard inversion (r.h.s.), for September 2001 until September 2008 and 10° zonal bins for northern mid to low latitudes.

pattern. The differences towards ECMWF decrease, which could be due to the change of the resolution of the ECMWF analysis fields in February 2006, from 60 vertical levels up to 91 levels, and more important, due to the start of assimilating GPS RO data (December 2006) into the fields. This change in the generation of ECMWF data affects also the time series plots of Figure 5.10 and Figure 5.11, leading to smaller differences predominately in the years 2007 and 2008.

A similar pattern of relative differences could be observed for the southern hemisphere, which is why it is not shown here. Furthermore, Figure 5.9 illustrated that below 35 km the two retrieval schemes are almost identical, leading together with the results from Figure 5.10 to Figure 5.12 to the conclusion that main differences between the two processing methods arise exclusively at higher latitudes and altitudes. The seasonally varying differences to ECMWF for the standard retrieval are probably due to problems with the SO. The seasonal bias of the new approach points most likely to problems with the ionosphere. The disadvantage of using observational data up to higher altitudes is that the residual influence of the ionosphere is increased, which could lead to such a bias. In that respect, further investigations are definetly necessary.

5.3.2 Comparison of CHAMP and COSMIC satellite data

In this section differences between the CHAMP and COSMIC satellite missions are studied, comparing the average bending angle approach with the standard retrieval. The goal is to understand on the one hand, systematic differences between CHAMP and COSMIC satellite data, and on the other hand, differences introduced through the retrieval method. The smoothing of noisy bending angles through averaging or statistical optimization can have different implications on the monthly refractivity climatologies, depending if satellite missions are noisier or not. So the question is also, apart from a systematic difference, which retrieval method provides more similar results between the two satellite missions. For that, the two missions are studied for an overlap period from September 2006 until December 2007.

As an initial analysis, Figure 5.13 shows relative differences between 10° zonal refractivity fields to co-located ECMWF fields for both missions (columns) and retrieval schemes (rows), studied for the northern latitude band 80°N to 90°N. It is noticeable, that the COSMIC data sets, computed with the standard retrieval show although COSMIC data is less noisy than CHAMP data, surprisingly the largest differences to ECMWF (left bottom), in contrast to the other plots. The results for CHAMP data, look relatively similar comparing the two retrieval methods (right column). Furthermore, as discussed in Subsection 5.3.1, there is a clear winter polar signal for the standard retrieval, especially for COSMIC data.

In order to get a better understanding of these results, I did a systematic analyzes of differences between retrieval schemes and satellite missions. Figure 5.14 studies the relative differences between monthly refractivites computed with CHAMP and COSMIC data, comparing new (left column) and standard retrieval (right column), from northern high latitudes down to low latitudes. The plots show decreasing refractivity differences between the two data sets towards low latitudes, while maximum values occur at high latitudes and altitudes. Comparing the new inversion (left) with the standard inversion (right) we observe for the latitude band 60°N to 70°N down to 0° to 10°N, very similar results between the two methods, indicating a real true difference between the two satellite missions. Only for the highest studied latitude band (80°N to 90°N) the pattern between the two methods differs. Since in that area the influence of the retrieval method is the highest, it is not surprising, that a systematic difference is overshadowed by technical diversities of the method.

Finally, in Figure 5.15 the differences between new and standard inversion are studied for northern high latitudes down to low latitudes, comparing CHAMP (left column) and COSMIC (right column) data sets. The refractivity differences show a similar pattern for both columns, presenting an increasing magnitude with increasing altitude and latitude. At high latitudes larger magnitudes extent down to lower altitudes (about 35 km), while

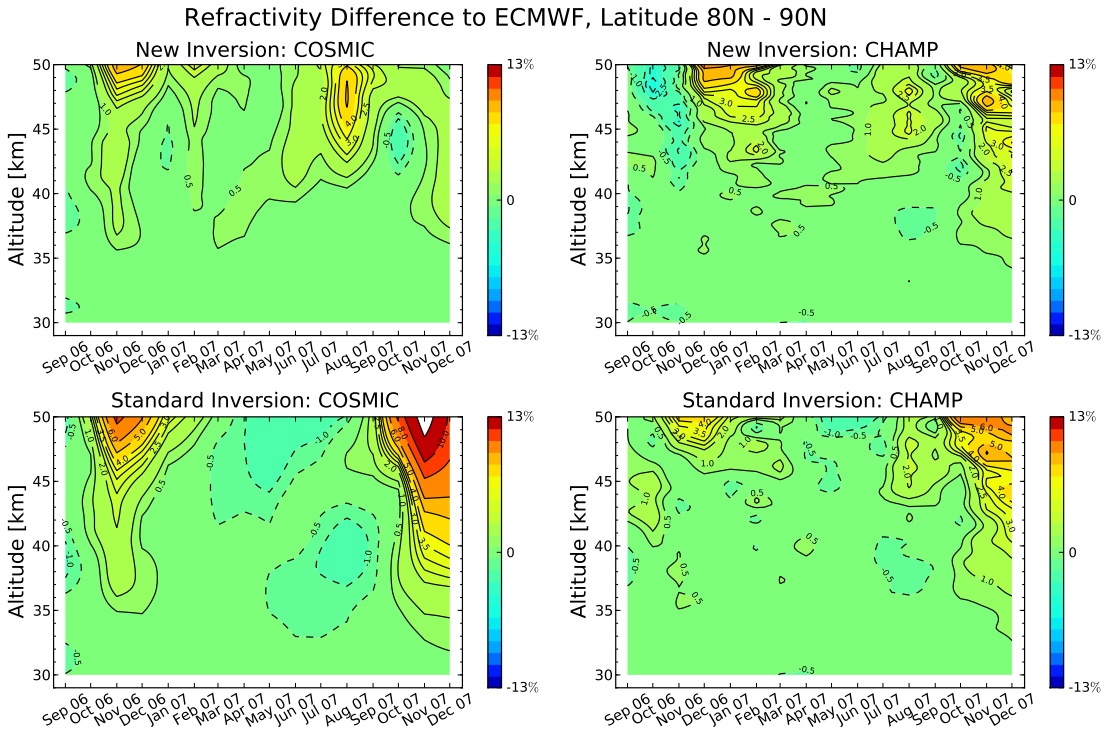

Figure 5.13: The left column shows the relative difference between monthly mean refractivity from COSMIC data and from collocated ECMWF data, comparing new inversion (top) and standard inversion (bottom), while the right column studies the difference between CHAMP data and collocated ECMWF data.

at low latitudes the magnitudes are even at altitudes of about 45 km small. For northern mid to high latitude winter months the differences are negative, while for northern non-winter months we find positive differences, with a maximum in northern summer. On the southern hemisphere the pattern is simply switched in sign, which is why it is not presented here. The differences increase up to about 2%, in case of CHAMP data, while the COSMIC data sets show larger differences between the two retrieval methods (up to about 4%). The larger differences in case of the COSMIC satellite mission are intuitively not expected, but can be explained due to differences in the processing for different RO missions in the SO retrieval scheme at the DMI. The CHAMP data were processed with SO parameter settings where the attempt was to minimize the impacts during southern hemisphere winter, whereas the COSMIC data were processed with an older set of SO parameter settings which had some known problems. The impact of the background information was set higher for the COSMIC mission than for the CHAMP mission, which results in larger differences between the two retrieval methods for COSMIC data sets, or in larger differences towards ECMWF data (see Figure 5.13, bottom left).

Summarizing the complete section, the new averaging approach showed very encouraging results, which suggest that for the study of climatologies it is also applicable to CHAMP data. The refractivity data from the averaging approach appear to agree slightly better with the co-located ECMWF analysis data than the standard retrieval. Furthermore, when comparing CHAMP and COSMIC data sets for the two retrieval methods, it seems that a real true systematic difference between the two satellite missions could be observed. The retrieval dependent errors seem only at high altitudes and latitudes to take overhand, and studied refractivity profiles start to depend more strongly on the applied retrieval scheme.

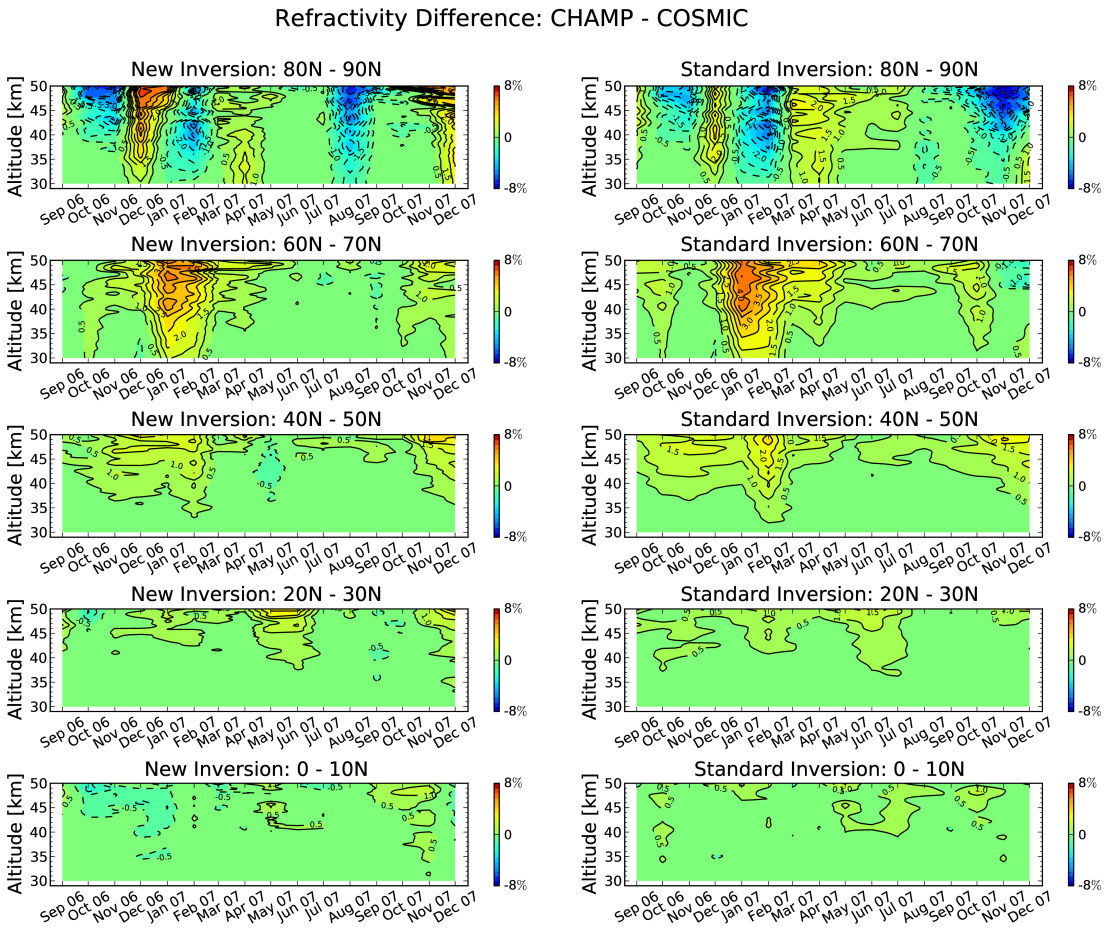

Figure 5.14: Relative differences between CHAMP and COSMIC monthly mean refractivities, comparing new (left column) and standard (right column) inversion, studied for northern higher to lower 10° latitude bands (top to bottom).

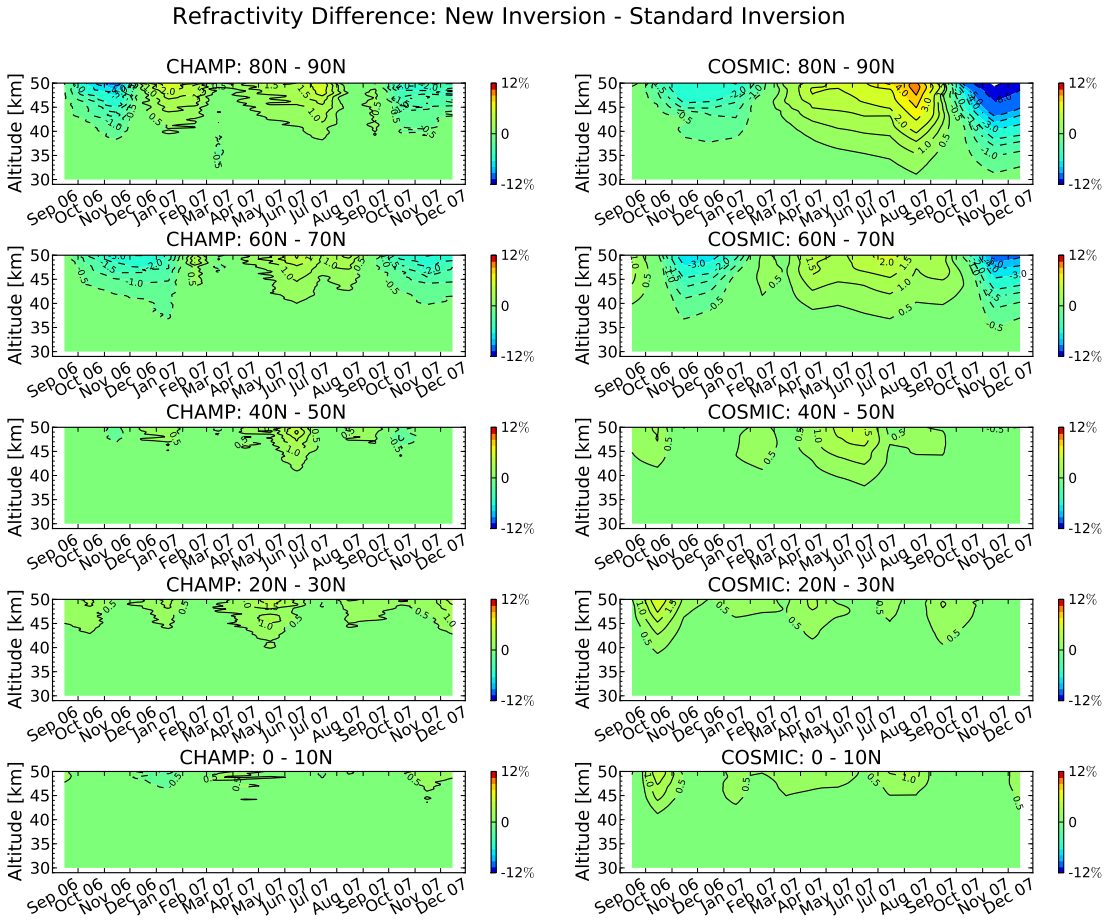

Figure 5.15: Relative differences between new inversion and standard inversion monthly mean refractivities, comparing CHAMP (left column) and COSMIC (right column) data sets, studied for northern higher to lower 10° latitude bands (top to bottom).

6 Summary, conclusions, discussions and outlook

In this study the idea of forwarding bending angle climatologies, instead of SO single bending angle profiles, through an Abel transformation, was tested on CHAMP data. It has been shown that SO is a source of structural uncertainty between different processing centers (Steiner et al. 2013), which may be circumvented by averaging primarily in bending angle space. An initial analysis of the average bending angle approach has been performed on COSMIC satellite data (Ao et al. 2012; Gleisner and Healy 2013). However, in order to obtain long-term climate data products the use of CHAMP data is also required. Since the CHAMP satellite mission has a reduced number of occultations compared to the COSMIC mission, and an increased noise level, it was questionable if the approach is also successful on CHAMP data.

I started the analyzes by studying 10° monthly zonal bending angle profiles, comparing bending angle means and medians. Due to large-scale wiggles in the mean value, I introduced an additional bending angle outlier rejection for values larger or smaller than $\pm 30\,\mu$rad between an altitude of 50 km to 80 km. The outlier rejection achieved smoother average bending angle profiles. The final average bending angle profiles were built from a combination between the mean and median bending angle values, similar to Gleisner and Healy (2013).

After performing the Abel transformation on the average bending angle profiles, monthly zonal refractivities were studied, leading to the firm conclusion that the average bending angle approach is also applicable to CHAMP data. The average profile processing and the single profile processing produce monthly mean refractivity climatologies which are nearly identical up to an altitude of 35 km, see Figure 5.9. Between 35 km to 50 km the differences between the two retrieval methods start to increase with increasing latitude, up to about 2% for high northern latitudes and CHAMP data, see Figure 5.15.

One of the research questions concerned problems of the standard retrieval at high altitudes and high latitude winter conditions, aiming better data quality with the new retrieval in that area and season. By analyzing differences of monthly mean refractivities relative to co-located ECMWF data on a longer time scale, I could detect a clear signal of increased differences towards ECMWF at high latitudes in the winter time for the standard

retrieval. The new retrieval showed an improvement of the refractivity climatologies relative to ECMWF in that region, with however slightly larger deviations for non-winter months compared to the standard retrieval. The results of the average bending angle approach are still encouraging, since the agreement with ECMWF is slightly better (see Figure 5.10 and Figure 5.11). Furthermore, the analyzed differences relative to ECMWF for mid to low latitudes, comparing new and standard retrieval (Figure 5.12), showed practically identical results, indicating a robustness among the choice of the approach at mid to low latitudes.

However, the slightly increased bias of the new approach relative to ECMWF data for non-winter months at high latitudes and the seasonal bias at mid to low latitudes, point to some remaining problems with the averaging approach. Most likely the problems arise from residual ionospheric errors, which are increased due to using observational data up to higher altitudes. The standard approach tries to handle this problem when using the SO, which as we know, introduces new problems, illustrated in the bias findings for the standard approach. Although there is a general interest in handling the problem of residual ionospheric errors, in case of the averaging approach, the residual influence of the ionosphere needs definetly to be investigated, e.g., similar to the study of Danzer et al. (2013).

Nevertheless, for the application of climatologies, the new approach showed some very promising results. Since up to 80 km altitude it is free of a priori information, the resulting climatology might can be used as a reference data set to profiles generated by the standard approach from different processing centers. To test that possibility, it would be interesting to compare new approach climatologies generated by different processing centers. The processing centers differ in their quality control. If the resulting climatology differences are small, it would mean that the new approach shows a robustness among processing centers which recommends it as a reference profile.

As a next step I propose to test limits of the approach on different spatial or maybe even temporal climatologies. So far 5° zonal bins on COSMIC data and 10° zonal bins on CHAMP and COSMIC data sets, on a monthly basis, have been tested. I suggest to test further longitudinal binning, e.g., 60°×10° longitudinal × latitudinal bins, or testing a two week time scale on zonal bins. If the averaging approach starts to fail with other binning choices it means one is rather restricted to a fixed climatology with that approach.

I conclude that it is possible to retrieve monthly refractivity profiles directly from averaged bending angles, using RO data from the CHAMP satellite mission. At that point the investigations showed very positive results which opened the door to a valid way of circumventing the SO step in climatological studies. Further necessary investigations have been pointed out and discussed, which should clarify limits and possibilities of the new approach.

Acknowledgments

I would like to thank Hans Gleisner and Kent B. Lauritsen (DMI) for making it possible to perform this visiting scientist activity. Especially I am grateful to Hans Gleisner for his support and help. The discussions were always fruitful, motivating and encouraging.

List of Figures

References

Ao, C. O., A. J. Mannucci, and E. R. Kursinski (2012). "Improving GPS Radio Occultation Stratospheric Refractivity Retrievals for Climate Benchmarking." *Geophysical Research Letters* 39.L12701. DOI: 10.1029/2012GL051720 (cit. on pp. 6, 11, 45).

Danzer, J., B. Scherllin-Pirscher, and U. Foelsche (2013). "Systematic residual ionospheric errors in radio occultation data and a potential way to minimize them." *Atmospheric Measurement Techniques* 6.8, pp. 2169–2179. DOI: 10.5194/amt-6-2169-2013. URL: http://www.atmos-meas-tech.net/6/2169/2013/ (cit. on p. 46).

Fjeldbo, G., A. J. Kliore, and V. R. Eshleman (1971). "The neutral atmosphere of Venus as studied with the Mariner V radio occultation experiments." *The Astronomical Journal* 76.2, pp. 123–140. DOI: 10.1086/111096 (cit. on p. 6).

Foelsche, U. and B. Scherllin-Pirscher (2011). *Development of bending angle climatology from RO data*. Tech. rep. CDOP Visiting Scientist Report 14. Ref: SAF/-GRAS/DMI/REP/VS14/001: GRAS-SAF, p. 51 (cit. on pp. 7, 14).

Foelsche, U., G. Kirchengast, A. K. Steiner, L. Kornblueh, E. Manzini, and L. Bengtsson (2008). "An observing system simulation experiment for climate monitoring with GNSS radio occultation data: Setup and test bed study." *Journal of Geophysical Research* 113, D11108. DOI: 10.1029/2007JD009231 (cit. on p. 11).

Gleisner, H. and S. B. Healy (2013). "A simplified approach for generating GNSS radio occultation refractivity climatologies." *Atmospheric Measurement Techniques* 6.1, pp. 121–129. DOI: 10.5194/amt-6-121-2013. URL: http://www.atmos-meas-tech.net/6/121/2013/ (cit. on pp. 5, 6, 11, 12, 15, 29, 45).

Gobiet, A. and G. Kirchengast (2004). "Advancements of Global Navigation Satellite System radio occultation retrieval in the upper stratosphere for optimal climate monitoring utility." *Journal of Geophysical Research* 109, D24110. DOI: 10.1029/2004JD005117 (cit. on p. 11).

Gorbunov, M. E. (2002). "Canonical transform method for processing radio occultation data in the lower troposphere." *Radio Science* 37.5. DOI: 10.1029/2000RS002592 (cit. on p. 10).

Gorbunov, M., K. Lauritsen, A Rhodin, M Tomassini, and L Kornblueh (2006). "Radio holographic filtering, error estimation, and quality control of radio occultation data." *Journal of geophysical research* 111.D10, p. D10105 (cit. on pp. 13, 24).

Ho, S.-P. et al. (2012). "Reproducibility of GPS radio occultation data for climate monitoring: Profile-to-profile inter-comparison of CHAMP climate records 2002 to 2008 from six data centers." *J. Geophys. Res.* 117, p. D18111. DOI: doi:10.1029/2012JD017665 (cit. on p. 10).

Kursinski, E. R., G. A. Hajj, J. T. Schofield, R. P. Linfield, and K. R. Hardy (1997). "Observing Earth's atmosphere with radio occultation measurements using the Global Positioning System." *Journal of Geophysical Research* 102, D19, pp. 23429–23465 (cit. on pp. 6, 10).

Scherllin-Pirscher, B. (2013). *Further development of BAROCLIM and implementation in ROPP*. Tech. rep. CDOP-2 Visiting Scientist Report 19. Ref: SAF/GRAS/DMI/REP/VS19/001: GRAS-SAF, p. 56 (cit. on p. 7).

Schwärz, M., B. Scherllin-Pirscher, G. Kirchengast, J. Schwarz, F. Ladstädter, J. Fritzer, and J. Ramsauer (2013). *Multi-Mission Validation by Satellite Radio Occultation*. Wegener Center, Uni Graz Final Report for ESA/ESRIN No. 01/2013 (cit. on p. 7).

Steiner, A. K., G. Kirchengast, U. Foelsche, L. Kornblueh, E. Manzini, and L. Bengtsson (2001). "GNSS occultation sounding for climate monitoring." *Physics and Chemistry of the Earth, Part A: Solid Earth and Geodesy* 26.3, D09102, pp. 113–124. DOI: 10.1016/S1464-1895(01)00034-5 (cit. on p. 10).

Steiner, A. K. et al. (2013). "Quantification of structural uncertainty in climate data records from GPS radio occultation." *Atmospheric Chemistry and Physics* 13.3, pp. 1469–1484. DOI: 10.5194/acp-13-1469-2013. URL: http://www.atmos-chem-phys.net/13/1469/2013/ (cit. on pp. 6, 10, 11, 45).

List of Acronyms

B

BAROCLIM Bending Angle Radio Occultation Climatology. 7, 34

C

CHAMP CHAllenging Mini-Satellite Payload. 5–9, 11–14, 19, 24, 25, 30, 31, 34, 36, 39, 40, 42, 45, 46, 48–50

COSMIC Constellation Observing System for Meteorology, Ionosphere, and Climate. 5–9, 11–13, 19, 24, 25, 31, 34, 39, 40, 42, 45, 46, 49, 50

D

DMI Danish Meteorological Institute. 5, 7, 9–11, 13, 24, 34, 40, 47

E

ECMWF European Centre for Medium-Range Weather Forecasts. 5–7, 9, 13, 14, 19, 22, 25, 31, 34, 36, 39, 40, 42, 45, 46, 48–50

EUMETSAT European Organisation for the Exploitation of Meteorological Satellites. 9

G

GFZ German Research Centre for Geosciences. 10

GNSS Global Navigation Satellite System. 10

GPS Global Positioning System. 6, 9, 36

M

MSIS Mass Spectrometer and Incoherent Scatter Radar. 6, 10, 11, 34

O

OCL Optimal Linear Combination. 10

Q

QC quality control. 24, 25

R

RO Radio Occultation. 5, 6, 9, 10, 36, 46

ROM Radio Occultation Meteorology. 9, 13, 34

ROPP Radio Occultation Processing Package. 9

S

SAF Satellite Application Facility. 9, 13, 34

SO Statistical Optimization. 5–7, 10, 11, 34, 39, 40, 45, 46

U

UCAR University Corporation for Atmospheric Research. 10

UCAR/CDAAC University Corporation for Atmospheric Research / Cosmic Data Analysis and Archive Center. 9

UTLS Upper Troposphere–Lower Stratosphere. 6